

Flight Control Design and Simulation Handling Qualities Assessment of High-Speed Rotorcraft

Tom Berger

Aerospace Engineer
Aviation Development Directorate
CCDC Aviation & Missile Center
Moffett Field, CA, USA

Chris L. Blanken

VM&C Tech Area Lead
Aviation Development Directorate
CCDC Aviation & Missile Center
Moffett Field, CA, USA

Mark B. Tischler

Senior Technologist
Aviation Development Directorate
CCDC Aviation & Missile Center
Moffett Field, CA, USA

Joseph F. Horn

Professor
Department of Aerospace Engineering
The Pennsylvania State University
University Park, PA, USA

ABSTRACT

The U.S. Army Aviation Development Directorate has developed generic high-fidelity flight-dynamics models of two advanced high-speed rotorcraft configurations—a lift offset coaxial helicopter with a pusher propeller and a tiltrotor. The models were developed to provide the government with independent control-system design, handling-qualities analysis, and simulation research capabilities for these types of aircraft in support of the Future Vertical Lift initiative. Full flight envelope explicit model following control systems were designed for both configurations using a multi-objective optimization approach to meet a comprehensive set of stability, handling qualities, and performance requirements. The control laws for both aircraft were evaluated in a piloted simulation experiment at the NASA Ames Vertical Motion Simulator using a series of high-speed handling qualities demonstration maneuvers. This paper discusses the control laws and the results of the piloted handling qualities assessment. The results from the simulation experiment show overall assigned Level 1 handling qualities for both aircraft.

INTRODUCTION

With the development of advanced high-speed rotorcraft, through the U.S. Department of Defense (DoD) Future Vertical Lift (FVL) initiative and Joint Multi-Role (JMR) Technology Demonstrator (TD) flight test program, new high-speed handling qualities requirements are needed to ensure safe and low-workload piloting in the transition and high-speed regimes. To provide the government with independent control-system design, handling-qualities analysis, and simulation research capabilities for advanced high-speed rotorcraft, the Aviation Development Directorate (ADD) has developed high-fidelity flight-dynamics models of generic versions of a lift offset coaxial helicopter with pusher propeller (herein referred to as coaxial-pusher) and tiltrotor aircraft. The aircraft mod-

eled fall under the FVL Capabilities Set #3. The models were developed using the comprehensive rotorcraft simulation code HeliUM (Refs. 1, 2), and are described in detail in Ref. 3. The models are generic in nature and not meant to represent specific aircraft (such as the SB>1 or V-280). A rendering of the models is shown in Figure 1.

To use the models for control system design and piloted simulations, linear models and trim data were extracted from HeliUM at different airspeeds, altitudes, and nacelle angles (in the case of the tiltrotor). The linear models were used to develop control system gain schedules using the Control Designer's Unified Interface (CONDUIT[®]) and design methods of Ref. 4. The control system for each aircraft was optimized to meet a wide range of stability, handling-qualities, and performance specifications throughout the flight envelope.

Once the control systems were developed, they were integrated with their respective bare-airframe models into full flight-envelope models that are capable of real-time simulation. The bare-airframe dynamics were modeled

Presented at the Vertical Flight Society 75th Annual Forum & Technology Display, Philadelphia, Pennsylvania, May 13–16, 2019. This is work of the U.S. Government and is not subject to copyright protection in the U.S. Distribution Statement A. Approved for public release; distribution is unlimited.

using a stitched model architecture (Refs. 5,6).

A piloted simulation experiment was conducted in the NASA Ames Vertical Motion Simulator (VMS) facility using five Army experimental test pilots (XPs). Since the focus of the experiment was high-speed and transition handling qualities, four newly developed National Rotorcraft Technology Center (NRTC) high-speed handling-qualities demonstration maneuvers were used: Pitch and Bank Attitude Capture and Hold (Ref. 7), Pitch and Roll Sum-of-Sines Tracking (Ref. 8), Break Turn (Ref. 9) and High-Speed Acceleration/Deceleration (Ref. 10).

The remainder of this paper will provide a brief overview of the coaxial-pusher and tiltrotor models. Following that, a description of the flight control systems for both aircraft will be given, including the architecture, design specifications, and optimization results. After a brief description of the simulation experimental setup, the results of the experiment will be provided first for the coaxial-pusher and then for the tiltrotor. This will be followed by a discussion of the results and conclusions.



(a) Coaxial-pusher



(b) Tiltrotor

Fig. 1. Generic aircraft schematics.

VEHICLE MODELS

The flight-dynamics models of the lift offset coaxial-pusher and tiltrotor configurations were developed using HeliUM-A, the U.S. Army Aviation Development Directorate (ADD) in-house flight-dynamics modeling

software tool developed as an extension to the University of Maryland HeliUM simulation model (Refs. 1,2). HeliUM-A uses a finite-element approach to model flexible rotor blades with coupled nonlinear flap/lag/torsion dynamics to capture structural, inertial, and aerodynamic loads along each blade segment, a key requirement for these advanced rotorcraft configurations. Blade, wing, and fuselage aerodynamics come from nonlinear lookup tables, and the rotor airwakes are modeled using a dynamic inflow model. A multi-body like modeling approach is used to build the aircraft configuration from its independent components (e.g., fuselage, wing, nacelle, etc.), which allows modeling of arbitrary aircraft configuration with multiple rotors.

The models are generic and are not meant to represent specific industry designs. Both aircraft have gross weights of roughly 32,000 lbs and fall into the FVL Capabilities Set #3 (previously known as FVL-Medium). The flight dynamics of both aircraft are modeled from hover to $V = 300$ kts, however, the maximum airspeeds of the models are limited to $V_H = 240$ kts for the coaxial-pusher and $V_H = 280$ kts for the tiltrotor using notional engine models.

The coaxial-pusher configuration was derived from a previous rotorcraft sizing trade-off study (Ref. 11), which gives the overall dimensional and weight characteristics as well as key rotor and aircraft aerodynamic properties. The generic tiltrotor configuration was derived from scaling geometric, inertial, and structural properties of the XV-15, V-22, and the notional NASA Large Civil Tilt-Rotor 2 (LCTR2). Berger et al. (Ref. 3) presents a detailed description of the coaxial-pusher and tiltrotor models.

Linear state-space point models and trim data were extracted from HeliUM-A at a range of airspeeds and altitudes. The linear models contain the rigid body states, the first two blade modes for each rotor (modeled as one collective, two cyclic, and one reactionless second-order rotor states), three (average, cosine, and sine) inflow states per rotor, as well as a pusher propeller inflow state for the coaxial-pusher and second-order nacelle angle dynamics for the tiltrotor. Overall the coaxial-pusher linear models contain 48 states and the tiltrotor linear models contain 51 states.

The linear point models were used to develop the flight control systems. Furthermore, the point models and trim data were combined to form continuous full-flight envelope quasi-linear parameter varying (qLPV) stitched simulation models (Ref. 5). These models were suitable for real-time simulation, and they formed the basis of the simulation models used in the experiment described here.

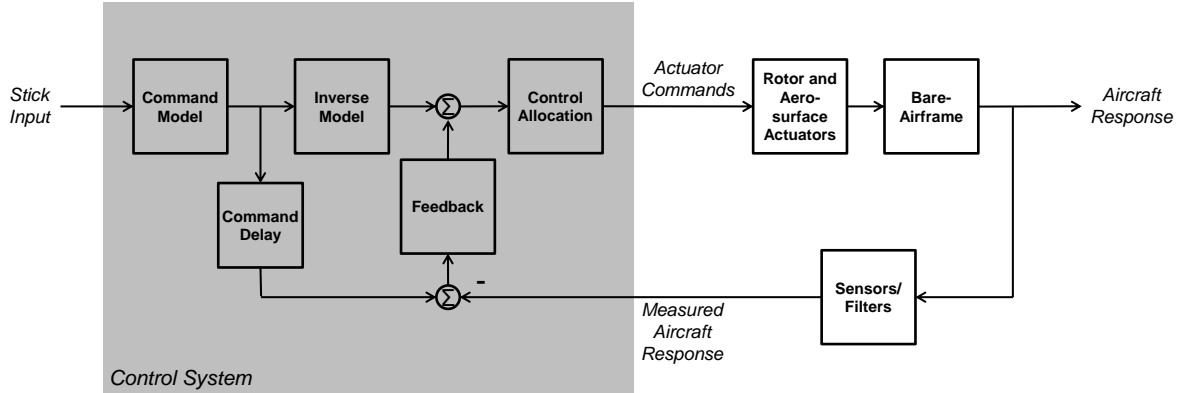


Fig. 2. Top level block diagram representation of control system.

FLIGHT CONTROL SYSTEMS

Full-flight envelope control systems were designed for both generic aircraft. This section describes the control system architecture, specification used to tune the control system parameters, and resulting predicted handling qualities.

Architecture

An explicit model following (EMF) control system architecture (Ref. 4) was used for both aircraft, shown in block diagram form in Figure 2. The control system consists of five main elements: 1) Control Allocation, 2) Command Model, 3) Inverse Model, 4) Command Delays, 5) Feedback. The following sections will describe each element in more detail.

Control Allocation A control allocation scheme is required for both the coaxial-pusher and tiltrotor aircraft, since both have redundant bare-airframe controls. Both aircraft have two sets of three main rotor swahsplate actuators (three per rotor). In addition, the coaxial-pusher has pusher propeller collective and lateral cyclic (monocyclic) actuators, as well as elevator and rudder actuators. In addition to its main rotor actuators, the tiltrotor has aileron and ruddervator actuators, as well as nacelle tilt actuators.

The control allocation scheme determines how to use the redundant bare-airframe controls most efficiently to achieve the pitch, roll, yaw, heave, and thrust commands generated by the pilot and control system. A weighted pseudo-inverse method (Refs. 12, 13) is used to allocate

the demanded roll, pitch, and yaw moments \mathbf{d} to each aircraft's control actuator commands \mathbf{u}_{cmd} :

$$\mathbf{u}_{\text{cmd}} = \mathbf{W}^{-1} \mathbf{B}_{\text{RB}}^T (\mathbf{B}_{\text{RB}} \mathbf{W}^{-1} \mathbf{B}_{\text{RB}}^T)^{-1} \mathbf{d} \quad (1)$$

where \mathbf{W} is a diagonal weighting matrix composed of the individual w_i weightings and \mathbf{B}_{RB} is the control effectiveness matrix, composed of the \dot{p} , \dot{q} , and \dot{r} rows of the rigid-body control derivative matrix. Berger, et al. (Ref. 3) provides a detailed description of the weighted pseudo inverse control allocation and demonstrates how it worked well to allocate demanded moments between the multiple rotor and aerosurface controls as flight condition varied.

Command Model The command model in each axis sets the aircraft response characteristics to pilot inputs (i.e., response type, magnitude, and bandwidth). Table 1 lists the response type in each axis as a function of airspeed.

In the roll axis, a Rate Command/Attitude Hold (RCAH) response type is used throughout the flight envelope, with a first-order command model given by:

$$\frac{p_{\text{cm}}}{\delta_{\text{lat}s}} = \frac{K_{\text{lat}}}{\tau_{\text{lat}}s + 1} \quad (2)$$

Note that rate command was chosen for the hover/low-speed to provide Level 1 handling qualities in a Good Visual Environment (GVE), however it is expected that an Attitude Command/Attitude Hold (ACAH) response type will be needed for Level 1 handling qualities in a Degraded Visual Environment (DVE) (Ref. 14). The EMF architecture used here provides the flexibility to easily change response types from rate command to attitude command for any future use of these control systems in DVE.

In the pitch axis, an RCAH response type is used between hover and $V = 200$ kts, with a first-order command model similar to the roll command model shown in Eq. 2. Above $V = 200$ kts, the response type changes to stability axes normal acceleration n_z command with angle of attack α hold, with a second-order command model given by:

$$\frac{n_{zcm}}{\delta_{lon_s}} = \frac{K_{lon} \omega_{lon}^2}{s^2 + 2\zeta_{lon} \omega_{lon} s + \omega_{lon}^2} \quad (3)$$

This is a typical fixed-wing response type (e.g., Ref. 15) which is useful for its simple ability to limit load factor and handle trim across a wide speed/loading range (trim $n_z = 1$ g regardless of speed/loading). As shown in Ref. 3, the bare-airframe dynamics of both the coaxial-pusher and tiltrotor aircraft have fixed-wing-like characteristics at high airspeed, and so fixed-wing response types at high speeds are a natural choice.

Between hover and $V = 100$ kts, pedals command yaw rate r , with a first-order command model similar to the roll command model shown in Eq. 2. In hover/low-speed, the hold mode on the pedals is direction (or heading) hold. The hold mode transitions to turn coordination above $V = 40$ kts. Above $V = 100$ kts, the response type commanded by the pedals changes to sideslip β command, with a second-order command model similar to the normal acceleration command model in Eq. 3. This is another response type typical of fixed-wing aircraft (e.g., Ref. 16), which has the benefits of easily limiting sideslip at high speed and providing automatic turn coordination.

Finally, the collective/thrust control lever (TCL) commands vertical speed with height (or altitude) hold between hover and $V = 40$ kts. Above $V = 40$ kts, the TCL is open-loop and provides a direct stick-to-head response.

Inverse Model The inverse model is used to generate actuator inputs that command the aircraft to approximately follow the command model responses, and is composed of lower-order inverses of the primary bare-airframe response in each axis. For each axis, the bare-airframe response of the commanded variable (listed in Table 1) is used. The lower-order inverse models are fit to the bare-airframe with the control allocation scheme included, such that a single-input/single-output (SISO) lower-order system is used for each axis.

For the tiltrotor roll rate p and yaw rate r responses, zeroth-order over first-order transfer function fits are used for all airspeeds, e.g., for roll:

$$\frac{p}{\delta_{lat}} = \frac{L_{\delta_{lat}}}{s - L_p} \quad (4)$$

For the coaxial-pusher, zeroth-order over first-order transfer function is used for the yaw rate r response and

roll rate p response at airspeeds above $V = 100$ kts. However, at airspeeds below $V = 100$ kts, a zeroth-order over first-order transfer function does not fit the bare-airframe roll rate response well. Figure 3 shows the coaxial-pusher bare-airframe roll rate p response to demanded rolling moment δ_{lat} in hover. The phase of the bare-airframe response flattens out at $\phi = -45$ deg between $\omega = 1 - 10$ rad/sec. This behavior is not captured by a zeroth-order over first-order fit as shown by the dashed red line in Figure 3. Therefore, a first-order over first-order fit:

$$\frac{p}{\delta_{lat}} = \frac{L_{\delta_{lat}}(s + 1/T_{\phi})}{s - L_p} \quad (5)$$

is used for the coaxial-pusher roll axis from hover to $V = 100$ kts (dashed green line in Figure 3).

For both aircraft, from hover to $V = 60$ kts, a zeroth-order over first-order transfer function fit is used for the pitch rate q response. Above $V = 60$ kts, the bare-airframe pitch rate response of both aircraft is better represented by a classical fixed-wing first-order over second-order transfer function:

$$\frac{q}{\delta_{lon}} = \frac{M_{\delta_{lon}}(s + 1/T_{\theta_2})}{s^2 + 2\zeta_{sp} \omega_{sp} s + \omega_{sp}^2} \quad (6)$$

For sideslip and normal accelerations responses, a zeroth-order over second-order transfer function fit is used.

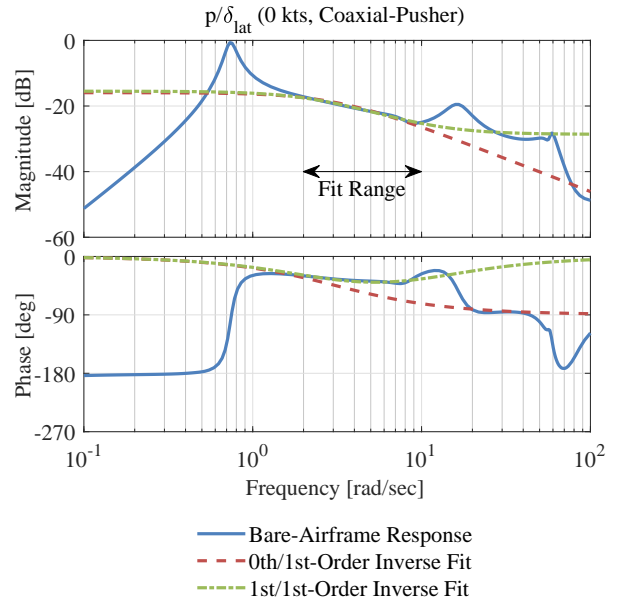


Fig. 3. Lateral axis inverse model fit (hover, coaxial-pusher).

Table 1. Control System Response Types

Speed Range [kts]	Lateral Cyclic	Longitudinal Cyclic	Pedals	Thrust Control Lever
0–40	Rate Command/ Attitude Hold	Rate Command/ Attitude Hold	Rate Command/ Direction Hold	Rate Command/ Height Hold
40–100			Rate Command/ Turn Coordination	Direct Stick to Head
100–200		Sideslip Command/ Turn Coordination		
200–300			Normal Acceleration Command/Angle of Attack Hold	

Command Delays Command delays τ_{cmd} are used to synchronize the commanded and actual states in time, before determining the error. The addition of command delays is typical in EMF control laws (Ref. 4), and is done to account for higher-order dynamics and delays from the actuators, sensors, filters, and flight control computer processing time that are not accounted for by the inverse model.

Accounting for this additional delay before comparing the commanded states with the actual states is useful to not overdrive the actuators. The addition of the command delays also reduces the amount of overshoot in the closed-loop end-to-end response with no added phase loss (Ref. 15).

Table 2 shows the command delay τ_{cmd} values in each axis for both aircraft. As expected, similar command delay values were determined for both aircraft. The tiltrotor does have slightly lower command delay values in the lateral and directional axes, due to the use of differential collective to generate roll and yaw moments.

Table 2. Command Delays

	Coaxial-Pusher	Tiltrotor
Axis	τ_{cmd} [sec]	τ_{cmd} [sec]
Lateral	0.12 – 0.14	0.1 – 0.11
Longitudinal	0.13 – 0.14	0.1 – 0.13
Directional	0.12 – 0.16	0.07 – 0.15
Vertical	0.04 – 0.06	0.04 – 0.09

Feedback Feedback is used to stabilize the aircraft, provide damping, account for inaccuracies in the lower-order inverse, minimize the error between the commanded response and actual aircraft response due to cross-coupling and other disturbances, and provide hold capabilities and disturbance rejection. Rate, attitude, and attitude integral feedback gains are used.

Table 3 lists the feedback gains used in each axis as a function of airspeed for both the coaxial-pusher and tiltrotor. A common set of feedback gains is used for both aircraft with two exceptions:

1. In the mid- to high-speed range ($V > 50$ kts), the tiltrotor uses roll rate (K_p) and roll attitude (K_ϕ) feedback only in the lateral axis as is typical of fixed-wing lateral-axis control laws (Ref. 16). However, the coaxial-pusher control systems additionally includes roll attitude integral feedback (K_{ϕ_I}). This is because large, rapid changes in thrust (and therefore torque) on the pusher propeller result in a sustained roll disturbance. Roll attitude integral feedback was extended to the entire airspeed range for the coaxial-pusher to counteract this disturbance and minimize pusher propeller thrust-to-roll coupling during sustained acceleration or deceleration.
2. The tiltrotor includes a lateral acceleration integral gain ($K_{n_{yl}}$) at high-speed ($V > 100$ kts), which is not used in the coaxial-pusher control systems. This gain was added to the tiltrotor control system to meet the turn coordination specification.

The feedback gains were optimized to meet a comprehensive set of stability, handling qualities, and perfor-

mance specifications using a multi-objective optimization approach in CONDUIT[®] (Ref. 4). The Specifications section below lists the specifications used for the optimization.

Actuators, Sensors, and Filters Accounting for all sources of time delays in the system is important during control system design and simulation testing to ensure that system performance is not pushed beyond what is capable. For this purpose, actuator, sensor, time delay, and filter models are included in both the linear control system design models as well as the nonlinear simulation models.

Rotor and aerosurface actuators are included in the block diagrams of both aircraft, and are represented by second-order systems with position and rate limits. Table 4 lists the actuator bandwidths and limits for the coaxial-pusher and tiltrotor actuators.

For both aircraft, the flight control computer (FCC) is assumed to be operating at 100 Hz. The FCC processing delay and digital-to-analog sample and hold delay are each accounted for by a half time-step ($\tau = 5$ msec) delay (Ref. 17), upstream of the actuator models.

Sensors are modeled as second-order systems with bandwidths of 5 Hz on all measured quantities. In addition, each sensor signal has a $\tau = 20$ msec delay, to account for sampling skew and bus transport delays.

Second order complementary filters are used on aero measurements airspeed V , angle of attack α , and angle of sideslip β . The filters combined direct measurements of these values at low frequency with estimates of their derivatives from inertial measurements at high frequency. Aero measurements are only used at high-speed ($V \geq 100$ kts).

Notch filters are used in the control system to avoid destabilizing the coupled fuselage rotor modes. For the coaxial-pusher, notch filters are used in the lateral axis ($\omega_n = 22$ rad/sec), in the longitudinal axis ($\omega_n = 12.5$ rad/sec), and in the directional axis ($\omega_n = 37$ rad/sec). These frequencies correspond to the coupled regressive flap/roll mode, coupled regressive flap/pitch mode, and differential collective lag mode, respectively. The locations of the rotor modes for the coaxial-pusher are shown as a function of airspeed in Figure 10 of Ref. 3. Similarly for the tiltrotor, notch filters are used in the lateral and longitudinal axes.

Specifications

A common, comprehensive set of stability, handling qualities, and performance specifications, shown in Table 5, was used to optimize both coaxial-pusher and tiltrotor control laws. The specifications were divided into

two categories—First Tier and Second Tier specifications (Ref. 4). First Tier specifications are key flight control and handling qualities requirements that drive the design optimization, and are guaranteed to be met for an optimized design. Second Tier specifications are those which are evaluated only at the end of the optimization. These are typically alternate requirements that give insight into the design and generally overlap with First Tier specifications. Because they are not evaluated during the optimization, due to computational time consideration, they are not always met.

First Tier Specifications For the coaxial-pusher and tiltrotor control laws, First Tier specifications were selected primarily from SAE AS94900 (Ref. 18) (stability margins) and ADS-33E (Ref. 14) (handling qualities requirements). For ADS-33E specifications with multiple boundaries based on the agility category MTE, boundaries for Aggressive Agility/Target Acquisition & Tracking were used.

Key First Tier specifications include absolute eigenvalue stability (EigLcG1), stability margins (StbMgG1), and Nichols margins (NicMgG1). These specifications ensure that the design is stable with sufficient stability margins for each control loop broken at the input to the control allocation matrix.

Standard stability margin boundaries of gain margin $GM \geq 6$ dB and phase margin $PM \geq 45$ deg (Ref. 18) are used throughout the flight envelope with two exceptions. First, for both aircraft in hover/low-speed, more strict stability margin requirements of $GM \geq 6.6$ dB and $PM \geq 50$ deg are enforced. This is to enable future development of nested outer velocity and position loops, which degrade inner-loop stability margins (Ref. 4). The second exception to the standard stability margin boundaries is for the coaxial-pusher longitudinal axis at airspeeds greater than $V = 260$ kts. Although $V_H = 240$ kts for this generic coaxial-pusher model, the control laws were designed up to $V = 300$ kts. As described in Ref. 3, the short-period mode of the coaxial-pusher is composed of two real poles, one of which is unstable. This pitch divergence becomes more unstable as airspeed increases, and the standard stability margin requirements cannot be met. Therefore, above $V = 260$ kts, $GM \geq 4$ dB and $PM \geq 40$ are enforced for the coaxial-pusher.

The model following cost specification (ModFoG2) compares the closed-loop frequency response in each axis with the frequency response of the command model. A cost function J_{MF} is computed based on the weighted difference in the magnitude and phase of the responses, and a value of $J_{MF} \leq 50$ is enforced, ensuring good command model following in each axis (Ref. 4).

Disturbance rejection bandwidth (DRB, DstBwG1) and

Table 3. Control System Feedback Gains

Speed Range [kts]	Lateral	Longitudinal	Directional	Vertical
0–40	K_p, K_ϕ, K_{ϕ_I}	$K_q, K_\theta, K_{\theta_I}$	K_r, K_ψ, K_{ψ_I}	$K_{V_z}, K_{V_{z_I}}$
40–100	$K_p, K_\phi, (K_{\phi_I})^*$		K_r	None
100–200		$K_\beta, K_{\dot{\beta}}, K_{\beta_I}, (K_{n_{y_I}})^\dagger$		
200–300			$K_{\dot{\alpha}}, K_\alpha, K_{n_{z_I}}$	

* Coaxial-pusher only

† Tiltrotor only

Table 4. Actuator Model Parameters

	Bandwidth [Hz]	Position Limit [deg]	Rate Limit [deg/sec]
<i>Both Aircraft</i>			
Main Rotor	8	±20	40
Elevator	8	±20	80
Rudder	8	±30	70
<i>Coaxial-Pusher Only</i>			
Pusher Prop. Collective	4	–10 – 100	5
Pusher Prop. Monocyclic	4	±10	20
<i>Tiltrotor Only</i>			
Aileron	8	±40	80
Collective Trim	8	0 – 35	5
Nacelle	1.5	0 – 95	8

peak (DRP, DstPkG1) specifications (Ref. 19) were enforced in each axis for the appropriate hold variable. For example, in the pitch axis DRB and DRP were enforced for pitch attitude below $V = 200$ kts, and for angle of attack for $V \geq 200$ kts.

A minimum crossover frequency specification (CrsMnG2) was included for each axis. This specification ensures that the frequency response for each control loop broken at the input to the control allocation

matrix has a crossover frequency above a specified value. The minimum crossover requirements are $\omega_{c_\phi} = \omega_{c_\theta} = 4.0$ rad/sec for roll and pitch, $\omega_{c_\psi} = 3.5$ rad/sec for yaw, and $\omega_{c_{V_z}} = 2.0$ rad/sec for heave. Setting the minimum crossover frequency is an alternate way to ensure the control system is robust to off-nominal configurations, rather than explicitly including many off-nominal models in the evaluation of every specification, which is computationally intensive for optimization. It is especially useful in model following control law architectures such as the one used here, since most of the handling qualities specifications can be met with a properly tuned command model and with less use of feedback. The attitude, sideslip, and vertical velocity integral gains ($K_{\phi_I}, K_{\theta_I}, K_{\psi_I}, K_{\phi_I}, K_{\beta_I}$, and $K_{V_{z_I}}$) were all constrained to their respective proportional gains using the minimum crossover frequency specification values in each axis. The ratio of integral (K_I) to proportional (K_P) gain was constrained to be:

$$\frac{K_I}{K_P} = \frac{\omega_c}{5} \quad (7)$$

which ensures that the integral gain is effective, without overly degrading phase margin (Ref. 4).

The Eigenvalue damping specification (EigDpG1) was used which evaluates the damping ratio of all closed-loop eigenvalues within a specified frequency range and compares them to the minimum required value.

The Open Loop Onset Point (OLOP, OlpOpG1) specification (Ref. 20) is included to evaluate the control law's

susceptibility to Pilot Induced Oscillations (PIOs) and limit cycle oscillations that can result from actuator rate limiting. Linear analysis methods ignore the nonlinear effects of actuator position and rate limiting. However, the OLOP specification is based on frequency domain describing function concepts, and is useful to include in the design process to not push the design beyond the actuator limits of the aircraft. Two OLOP specifications are used per axis for both piloted and disturbance inputs for this two degree-of-freedom EMF architecture (Ref. 4). Since both coaxial-pusher and tiltrotor aircraft have redundant actuators, the OLOP specification in each axis was evaluated for the most critical actuator at each air-speed (first actuator to reach a rate limit for stop-to-stop inputs).

Piloted bandwidth specifications from ADS-33E (BnwRoH1-FrqHeH1) were included in each axis with appropriate boundaries based on flight condition (hover/low-speed and forward flight). For the hover/low-speed yaw attitude bandwidth specification (BnwYaH1), the reduced boundaries from Ref. 21 were used.

For high-speed flight ($V > 100$ kts), the ADS-33E flight path response to pitch attitude specification was included (FlpPiF1). Enforcing this specification ensures that the flight path or vertical rate response does not lag the pitch attitude response by more than $\phi = 45$ deg at all frequencies below $\omega = 0.4$ rad/sec, which corresponds to a maximum flight path-attitude lag $T_{\theta 2} = 1.96$ sec.

In addition, maximum achievable rates specifications (MaxRoH3-MaxHeH3) were included (Ref. 14). Finally, a set of cross-coupling requirements from ADS-33E were included in the First Tier specifications (CouPRH2-CouCPF1).

Second Tier Specifications Second Tier specifications are used as “check only” and are not enforced by the control system optimization. In this case, Second Tier specifications include ADS-33E attitude quickness and requirements from the military fixed-wing handling qualities requirements MIL-STD-1797B (Ref. 22).

The ADS-33E attitude quickness specifications (QikRoH1-QikYaH2) are used as a check only for several reasons. First, it is a time domain specification which requires the computationally expensive simulation of the design model at each iteration of the control system optimization. Second, the results of this specification vary greatly with input shape, size, and duration, and would result in non-smooth gradients of the specification value with feedback gain selection, which is not a desirable characteristic in parametric optimization (Ref. 4). Target Acquisition & Tracking attitude quickness boundaries were used as an objective requirement, while the less stringent boundaries for All

Other MTEs were used as a threshold requirement. For the yaw axis, the reduced attitude quickness boundaries from Ref. 21 were used.

For the MIL-STD-1797B specifications, boundaries for Category A flight phase (nonterminal flight phases that require rapid maneuvering, precision tracking, or precise flight-path control) and Class I aircraft (high-maneuverability air vehicles) are used.

Specifications from MIL-STD-1797B primarily consist of lower-order equivalent systems (LOES) specifications. For these specifications which are typical of fixed-wing aircraft, a lower-order transfer function fit is made to the closed-loop aircraft response, and the parameters of this equivalent transfer function are then evaluated against the specification boundaries. In the lateral/directional axes, individual LOES fits of the roll rate p response to lateral stick δ_{lat_s} input and sideslip β response to pedal δ_{ped_s} input are used. The fits were made over the frequency range of $\omega = 0.1 - 10$ rad/sec, and the LOES transfer functions are (Ref. 23):

$$\frac{p}{\delta_{\text{lat}_s}} = \frac{L_{\delta_{\text{lat}_s}} e^{-\tau_{\phi} s}}{s + 1/T_r} \quad (8)$$

$$\frac{\beta}{\delta_{\text{ped}_s}} = \frac{Y_{\delta_{\text{ped}_s}} e^{-\tau_{\beta} s}}{s^2 + 2\zeta_{\text{dr}} \omega_{\text{dr}} s + \omega_{\text{dr}}^2} \quad (9)$$

Two individual fits are used, instead of a simultaneous fit, since the responses are decoupled by design of the control system. Specifications on equivalent roll mode time constant (T_r), Dutch roll damping and frequency (ζ_{dr} , ω_{dr}), and time delays (τ_{ϕ} , τ_{β}) are enforced (FrqRoD4-TdIYaD1).

In the longitudinal axis, simultaneous LOES fits of the pitch rate and normal acceleration responses to longitudinal stick input are used. The fits were made over the frequency range of 0.5-7 rad/sec, and the LOES transfer functions are (Ref. 23):

$$\frac{q}{\delta_{\text{lon}_s}} = \frac{M_{\delta_{\text{lon}_s}} (s + 1/T_{\theta 2}) e^{-\tau_{\theta} s}}{s^2 + 2\zeta_{\text{sp}} \omega_{\text{sp}} s + \omega_{\text{sp}}^2} \quad (10)$$

$$\frac{n_z}{\delta_{\text{lon}_s}} = \frac{Z_{\delta_{\text{lon}_s}} e^{-\tau_{n_z} s}}{s^2 + 2\zeta_{\text{sp}} \omega_{\text{sp}} s + \omega_{\text{sp}}^2} \quad (11)$$

Specifications on equivalent control anticipation parameter (CAP), short period damping (ζ_{sp}), and time delay (τ_{θ}) are enforced (CapPiL1 and TdPiL1).

A specification on LOES fit cost J_{LOES} is included (CosLoG1) to ensure the parameters of the LOES fit accurately represent the closed-loop aircraft dynamics. If the LOES fit cost is too high ($J_{\text{LOES}} > 50$), then the LOES specifications should not be evaluated.

In addition to the LOES specifications from MIL-STD-1797B listed above, five more specifications that do not

require an LOES fit are used. The first two are the pitch attitude (BnwPiL4) and flight path (BnwFpL1) bandwidth specifications, which are evaluated directly from the closed-loop frequency responses. The next three MIL-STD-1797B specification that do not require an LOES fit are the time domain specifications that enforce time to bank requirements (roll performance, RolPFD1), pitch attitude dropback (DrpPiL1), and maximum lateral accelerating during steady turns (turn coordination, Trn-CrD2).

Optimization Strategy

The control law parameters are gain scheduled as a function of airspeed for the coaxial-pusher. Parameters were determined at 10 kt increments from hover to $V = 300$ kts, for a total of 31 design points. For the tiltrotor, control law parameters are gain scheduled as a function of airspeed and nacelle angle. Figure 4 shows the tiltrotor design points (71 total design points), which are also in increments of 10 kts and span the conversion corridor.

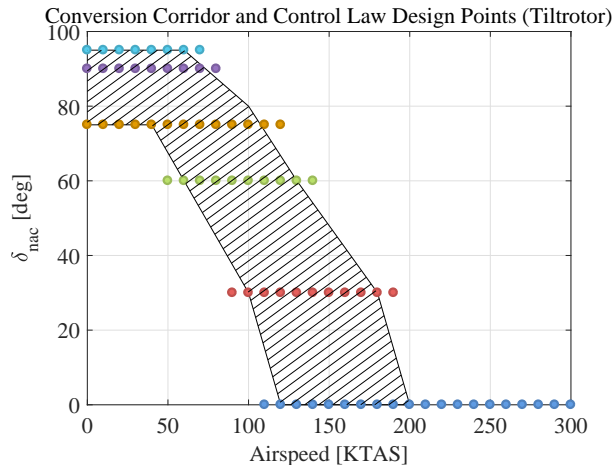


Fig. 4. Conversion corridor (hatched region) and gain schedule design points (tiltrotor).

At each design point, the command model parameters (stick gains and break frequencies) were hand-tuned to meet the piloted bandwidth, attitude quickness, and maximum achievable rate requirements. The parameters of the inverse model were determined from lower-order fits to the bare-airframe responses. The feedback gains listed in Table 3 were optimized in CONDUIT[®] using a multi-objective optimization approach to meet all of the Hard, Soft, and Summed Objective constraints (Ref. 4) listed in Table 5. At any given design point, between six and 11 feedback gains were optimized simultaneously to meet all of the requirements. The following sub-sections show

the control system optimization results for both configurations.

Optimization Results

Coaxial-Pusher Figure 5 shows the coaxial-pusher pitch rate (K_q) and angle of attack rate ($K_{\dot{\alpha}}$) feedback gains as a function of airspeed. Figure 6 shows the coaxial-pusher pitch attitude (K_θ) and angle of attack (K_α) feedback gains as a function of airspeed. Both figures demonstrate that CONDUIT[®] optimization resulted in smooth gain schedules. The only discontinuities are in changing response type from pitch rate command ($V < 200$ kts) to normal acceleration command ($V > 200$ kts), and from relaxing the stability margin requirements above $V = 260$ kts. The remaining feedback gains show similar trends.

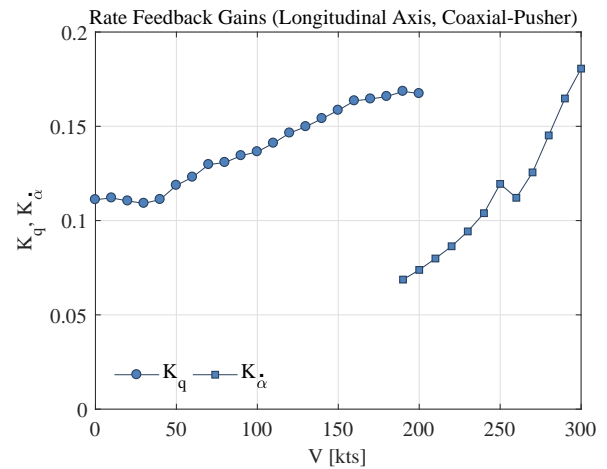


Fig. 5. Pitch rate and angle of attack rate feedback gains (coaxial-pusher, optimized designs).

Figures 7 and 8 show several of the First and Second Tier specifications and the optimized design values for several airspeeds ranging from hover to $V = 240$ kts. Figure 7 shows the stability margin, minimum crossover frequency, DRB/DRP, and OLOP specifications in all four axes. These are all First Tier specifications, and so they are met for all designs through the optimization process. Several observations can be made:

- In the roll and yaw axes (Figure 7, first and third columns), stability margins are lowest in hover, and increase as airspeed increases. In contrast, in the pitch axis (Figure 7, second column), the stability margins decrease as airspeed increases. At $V = 240$ kts (purple point), the pitch stability margins are in the corner of the stability margin requirement. This indicates that further reduction in phase margin cannot be counteracted by the addition of a lead-lag

Table 5. Control System Optimization Specifications

CONDUIT®					
Spec Name	Description (Motivation)	Axis*	Speed Range [kts]	Source	
<i>Hard Constraints (Stability Requirements)</i>					
EigLcG1	Eignevalues in L.H.P. (Stability)	All	All	Generic	
StbMgG1	Gain Phase Margin broken at elevator (Stability)	All	All	AS94900	
NicMgG1	Nichols Margins broken at elevator (Stability)	All	All	GARTEUR	
<i>Soft Constraints (Handling Qualities Requirements)</i>					
ModFoG2	Command model following cost (HQ)	All	All	Generic	
DstBwG1	Dist. Rej. Bandwidth (Loads, Ride Quality)	All	All	Ref. 19	
DstPkG1	Dist. Rej. Peak (Loads, Ride Quality)	All	All	Ref. 19	
CrsMnG2	Minimum $\omega_c \geq 4.0$ rad/sec (Robustness)	P,R	All	Generic	
	Minimum $\omega_c \geq 3.5$ rad/sec (Robustness)	Y	All	Generic	
	Minimum $\omega_c \geq 2.0$ rad/sec (Robustness)	H	0-40	Generic	
EigDpG1	Eigenvalue Damping (HQ, Loads)	All	All	Generic	
OlpOpG1	Open Loop Onset Point, pilot input (PIO)	All	All	DLR	
OlpOpG1	Open Loop Onset Point, disturbance input (PIO)	All	All	DLR	
BnwRoH1	Roll attitude bandwidth and phase delay, hover (HQ)	R	0-60	ADS-33E	
BnwRoF1	Roll attitude bandwidth and phase delay, forward flight (HQ)	R	60-300	ADS-33E	
BnwPiH1	Pitch attitude bandwidth and phase delay, hover (HQ)	P	0-60	ADS-33E	
BnwPiF1	Pitch attitude bandwidth and phase delay, forward flight (HQ)	P	60-300	ADS-33E	
BnwYaH1	Yaw attitude bandwidth and phase delay, hover (HQ)	Y	0-60	ADS-33E [†]	
BnwYaF1	Yaw attitude bandwidth and phase delay, forward flight (HQ)	Y	60-300	ADS-33E	
FrqHeH1	Heave response equivalent time constant, delay (HQ)	H	0-40	ADS-33E	
FlpPiF1	Flight path response to pitch attitude (HQ)	H	100-300	ADS-33E	
MaxRoH3	Maximum achievable roll rate, hover (HQ)	R	0-60	ADS-33E	
MaxRoF4	Maximum achievable roll rate, forward flight (HQ)	R	60-300	ADS-33E	
MaxPiH3	Maximum achievable pitch rate, hover (HQ)	P	0-60	ADS-33E	
MaxPiF1	Maximum achievable load factor, forward flight (HQ)	P	60-300	ADS-33E	
MaxYaH3	Maximum achievable yaw rate, hover (HQ)	Y	0-60	ADS-33E	
MaxHeH3	Maximum achievable vertical rate, hover (HQ)	H	0-40	ADS-33E	
CouPRH2	Pitch-roll coupling (HQ)	P,R	All	ADS-33E	
CouYaH1	Yaw-collective coupling, hover (HQ)	Y,H	0-60	ADS-33E	
CouCPF1	Pitch-heave coupling, forward flight (HQ)	P,H	40-300	ADS-33E	
<i>Summed Objective (Performance Requirements)</i>					
CrsLnG1	Crossover Frequency (Act. Activity)	All	All	Generic	
RmsAcG1	Actuator RMS (Act. Activity)	All	All	Generic	
<i>Check Only</i>					
Second Tier	QikRoH1	Roll attitude quickness, hover (HQ)	R	0-60	ADS-33E
	QikRoF1	Roll attitude quickness, forward flight (HQ)	Y	60-300	ADS-33E
	QikPiH1	Pitch attitude quickness, hover (HQ)	P	0-60	ADS-33E
	QikYaH2	Yaw attitude quickness, hover (HQ)	Y	0-60	ADS-33E [†]
	FrqRoD4	LOES Roll model time constant (HQ)	R,Y	60-300	MIL-STD-1797B
	FrqDrD3	LOES Dutch roll frequency (ω_{dr}) (HQ)	R,Y	60-300	MIL-STD-1797B
	DmpDrD2	LOES Dutch roll damping (ζ_{dr}) (HQ)	R,Y	60-300	MIL-STD-1797B
	TdlRoD1	LOES Roll axis time delay (HQ)	R,Y	60-300	MIL-STD-1797B
	TdlYaD1	LOES Yaw axis time delay (HQ)	R,Y	60-300	MIL-STD-1797B
	CapPiL1	LOES Control Anticipation Parameters (HQ)	P	60-300	MIL-STD-1797B
	TdlPiL1	LOES pitch axis time delay (HQ)	P	60-300	MIL-STD-1797B
	CosLoG1	Max LOES Cost ($J \leq 10$) (HQ)	P,R,Y	60-300	Generic
	BnwPiL4	Bandwidth, phase delay (HQ)	P	60-300	MIL-STD-1797B
	BnwFpL1	Transient flight-path response (HQ)	P	60-300	MIL-STD-1797B
	RoLPfD1	Time to achieve bank angle (HQ)	R	60-300	MIL-STD-1797B
	DrpPiL1	Pitch dropback (HQ)	P	60-300	MIL-STD-1797B
	TrnCrD2	Turn coordination max n_y (HQ)	R,Y	60-300	AS94900

* R = Roll, P = Pitch, Y = Yaw, H = Heave

[†] Reduced boundaries from Ref. 21 used

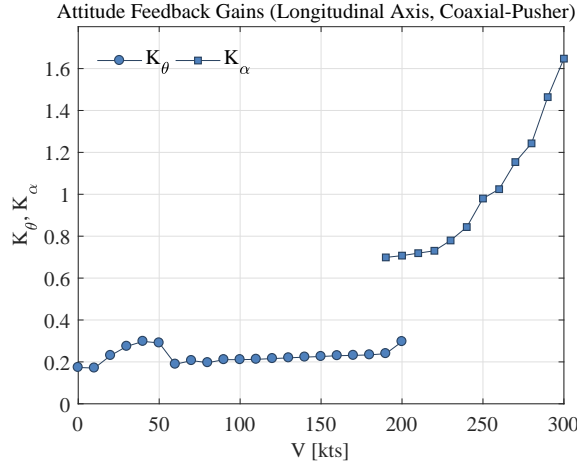


Fig. 6. Pitch attitude and angle of attack feedback gains (coaxial-pusher, optimized designs).

filter, since there is no gain margin to trade off for phase margin. And vice versa for further reduction in gain margin. Thus the relaxation of the longitudinal stability margin requirements above $V = 260$ kts.

- The resulting crossover frequencies ω_c in each axis are on the Level 1/Level 2 boundaries of their respective minimum crossover frequency specifications. This is a result of the optimization approach used in CONDUIT[®], where the specifications are met with the minimum use of the actuators (i.e., the Pareto optimal solution) (Ref. 4).
- The roll and pitch DRB requirements were optimized using a design margin of 110%, resulting in the values being above the minimum required boundaries (Figure 7, third row, first and second subplots).
- The yaw axis OLOP specification is closest to the Level 1/Level 2 boundary in the low- to mid-air speed range ($V = 60$ kts). This is because in this airspeed range the yaw control power of the coaxial-pusher is limited as differential torque on the rotors becomes less effective at generating yawing moment and the rudders have not become fully effective yet. For this reason, pusher propeller monocyclic is used in this airspeed range as described in Ref. 3.

Figure 8 shows the piloted bandwidth/phase delay and maximum achievable rates for roll, pitch, and yaw (first two rows). These are First Tier requirements and are met for all designs through the optimization process and tuning of the command models. The last two rows of specification in Figure 8 are all Second Tier requirements. Recall that these requirements are not enforced during the optimization, but are simply checked afterward. The third row of specifications in Figure 8 shows the atti-

tude quickness specification for roll, pitch, and yaw. The roll hover/low-speed and mid-/high-speed specifications (Figure 8, third row, first two subplots) display two sets of boundaries. The gray dashed boundaries represent the Target Acquisition & Tracking attitude quickness requirement (used as an objective requirement), while the solid black boundaries represent All Other MTEs requirement (used as a threshold requirement). The low ($V < 60$ kts) and high-speed ($V > 120$ kts) designs meet the Target Acquisition & Tracking boundaries, while the mid-speed designs ($V \approx 60$ kts) meet the All Other MTEs boundaries.

Pitch and yaw attitude quickness specifications (Figure 8, third row, third and fourth subplots) are available for hover/low-speed only. In the pitch axis, the designs meet the Target Acquisition & Tracking boundaries, while in the yaw axis the designs meet the All Other MTEs boundaries.

The last row of specifications shown in Figure 8 consists of MIL-STD-1797B requirements: (from left to right) pitch attitude bandwidth, flight path bandwidth, CAP, and pitch attitude dropback. The pitch attitude bandwidth requirement from MIL-STD-1797B (Figure 8, fourth row, first subplot) is similar to the pitch attitude bandwidth requirement from ADS-33E (Figure 8, first row, second subplot), but requires a higher minimum bandwidth ($\omega_{BW} \geq 3.0$ rad/sec versus $\omega_{BW} \geq 2.0$ rad/sec) and has a lower maximum allowable value of phase delay. The MIL-STD-1797B requirement is geared towards faster-flying aircraft than the ADS-33E requirement, and might be more applicable to new advanced rotorcraft configurations with maximum speeds significantly faster than those of the legacy helicopters used to validate the ADS-33E specification boundaries.

The CAP requirement (Figure 8, fourth row, third subplot) is evaluated based on an LOES fit (Eqs. 10 and 11) of the closed-loop aircraft response. Note that the longitudinal LOES requirements were only evaluated for $V > 100$ kts, where the LOES fit cost was below $J_{LOES} = 50$. Although the CAP value is within the Level 1 requirement for all airspeeds, the equivalent short period damping ζ_{sp} is slightly too high for the mid-air speed range, and is $\zeta_{sp} \geq 1.0$ for all airspeeds. A damping ratio $\zeta_{sp} > 1.0$ is expected for the RCAH designs ($V < 200$ kts) because the pitch command model, and therefore aircraft pitch rate response, is shaped like a first-order response. Therefore, the closed-loop transfer function in Eq. 10 must fit a first-order response, which happens when the denominator splits into two real poles, one at the command model break frequency and one canceling the bare-airframe $1/T_{\theta_2}$ zero. Although this may seem like an under-constrained fit (due to this pole-zero cancellation), the pole being canceled is constrained by the simultaneous fit of the normal acceleration response which does

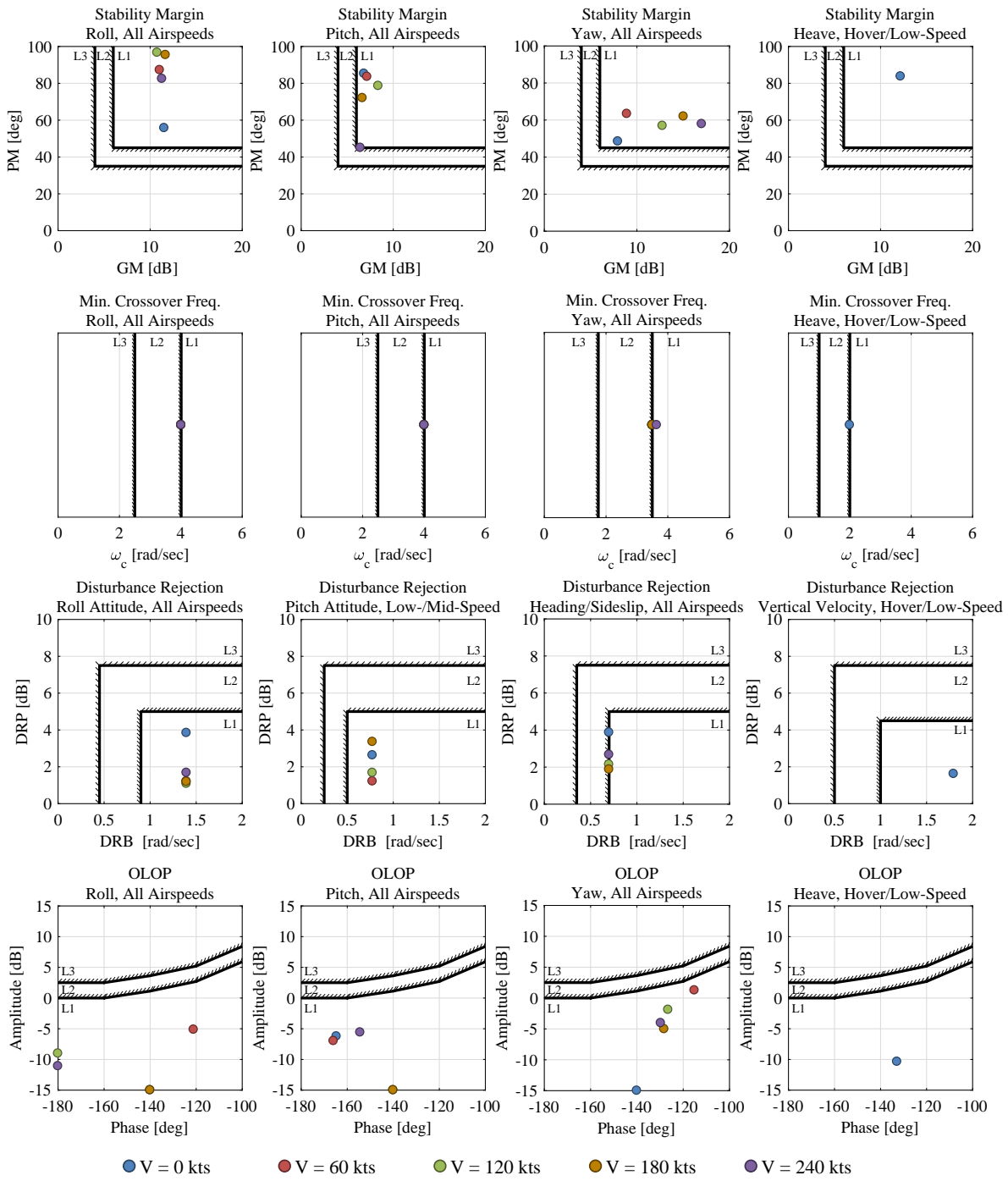


Fig. 7. Example control system design specification and optimized design results (1/2, Coaxial-Pusher, hover–240 kts).

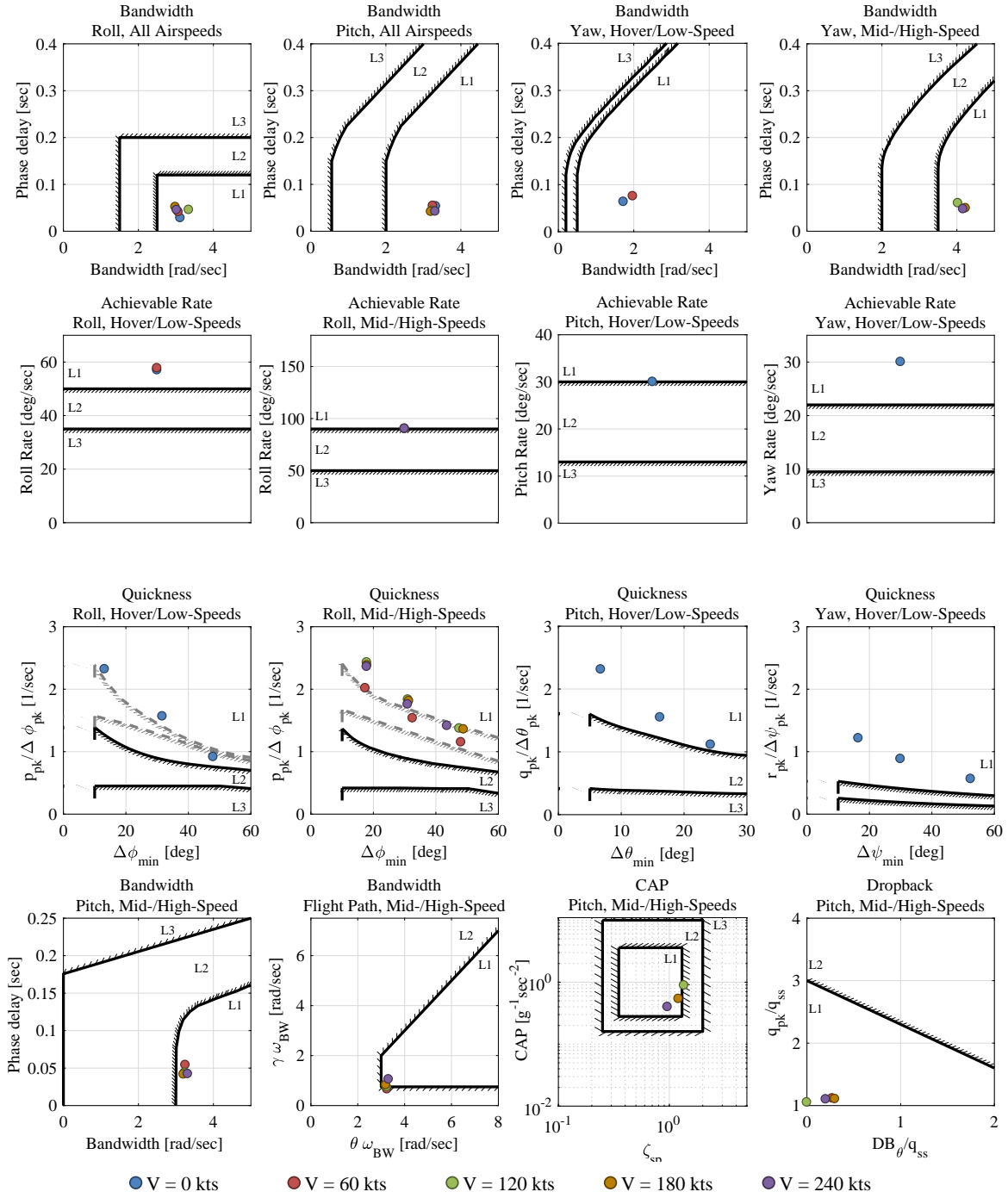


Fig. 8. Example control system design specification and optimized design results (2/2, Coaxial-Pusher, hover-240 kts).

not have a zero in its transfer function fit (Eq. 11). The resulting large ζ_{sp} indicated that either this requirement is not applicable to this response type, or that a higher-order pitch command model, similar to a classical bare-airframe response (Eq. 10) may be needed to provide good handling qualities at higher airspeeds. Note that for normal acceleration n_z command portion of the ($V > 200$ kts), the normal acceleration command model is second order (matches the form of the transfer function in Eq. 11) and therefore the response is similar to a classical aircraft response. For this response type, the CAP requirement is applicable and is met for the coaxial-pusher.

Finally, the dropback requirement is shown in the last subplot in Figure 8 and is met for all design conditions.

Tiltrotor Figure 9 shows the tiltrotor pitch rate (K_q) and angle of attack rate ($K_{\dot{\alpha}}$) feedback gains as a function of airspeed V and nacelle angle δ_{nac} (with $\delta_{nac} = 90$ deg corresponding to helicopter mode and $\delta_{nac} = 0$ deg corresponding to airplane mode). Figure 10 shows the tiltrotor pitch attitude (K_θ) and angle of attack (K_α) feedback gains as a function of airspeed V and nacelle angle δ_{nac} . Like for the coaxial-pusher, CONDUIT[®] optimization of the tiltrotor control laws resulted in smooth gain schedules. The remaining feedback gains show similar trends.

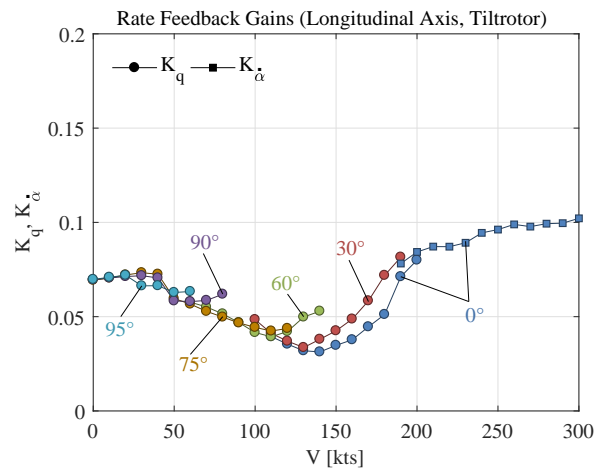


Fig. 9. Pitch rate and angle of attack rate feedback gains (tiltrotor, optimized designs).

Figures 11 and 12 show several of the First and Second Tier specifications and their values for several airspeeds ranging from hover to $V = 240$ kts. At each airspeed, the results are shown for the nacelle range spanning the conversion corridor shown in Figure 4, with the results for the different nacelle angles at each airspeed connected with lines.

Figure 11 shows the stability margin, minimum crossover frequency, DRB/DRP, and OLOP specifications in all

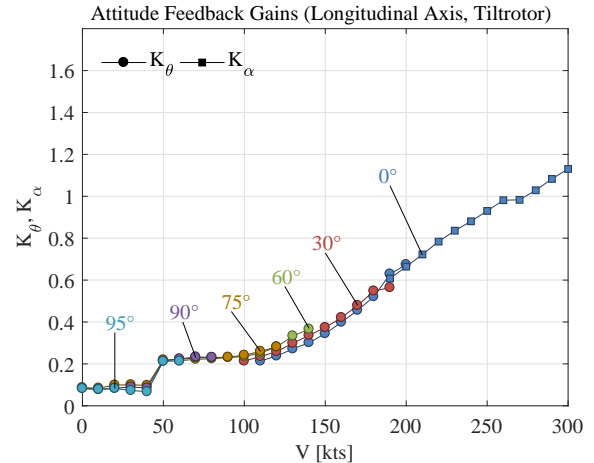


Fig. 10. Pitch attitude and angle of attack feedback gains (tiltrotor, optimized designs).

four axes. These are all First Tier specifications, and so are met for all designs through the optimization process. In the roll axis (Figure 11, first column), stability margin, minimum crossover frequency, and DRB/DRP are not strong functions of nacelle angle. However, The OLOP specification is a strong function of nacelle angle, with the values getting closer to the Level 1/Level 2 boundary for lower nacelle angles. This is because at lower nacelle angles, differential collective becomes less effective at generating roll moment, and differential longitudinal cyclic is phased in (Ref. 3). In contrast, the opposite is true for the yaw OLOP specification (Figure 11, last row, third subplot), where the values move away from the Level 1/Level 2 boundaries for lower nacelle angles as differential collective becomes more effective at generating yaw moment.

Figure 12 shows the piloted bandwidth/phase delay and maximum achievable rates for roll, pitch, and yaw (first two rows). These are First Tier requirements and are met for all designs through the optimization process and tuning of the command models.

The third row of specifications in Figure 12 shows the attitude quickness specification for roll, pitch, and yaw (Second Tier requirements). The roll hover/low-speed and mid-/high-speed specifications (Figure 12, third row, first two subplots) display two sets of boundaries. The gray dashed boundaries represent the Target Acquisition & Tracking attitude quickness requirement (used as an objective requirement), while the solid black boundaries represent All Other MTEs requirement (used as a threshold requirement). At airspeed below $V = 200$ kts, the roll attitude quickness values meet the Target Acquisition & Tracking boundaries for larger nacelle angles, and meet the All Other MTEs boundaries for smaller nacelle angles. This is consistent with the decreased roll control

power as the nacelles are lowered. In the high airspeed range (airplane mode), the ailerons are fully effective and roll control power is increased. The $V = 240$ kts design meets the Target Acquisition & Tracking roll boundaries.

Pitch and yaw attitude quickness specifications (Figure 12, third row, third and fourth subplots) are available for hover/low-speed only. In the pitch axis, the designs meet the Target Acquisition & Tracking boundaries, while in the yaw axis the designs meet the All Other MTEs boundaries.

The last row of specifications shown in Figure 12 consists of MIL-STD-1797B requirements: (from left to right) pitch attitude bandwidth, flight path bandwidth, CAP, and pitch attitude dropback. All of the designs meet the Level 1 pitch attitude bandwidth requirement from MIL-STD-1797B (Figure 12, fourth row, first subplot). However, some of the mid-speed designs ($60 < V < 120$ kts) have flight path bandwidth values that are in the Level 2 region (Figure 12, fourth row, second subplot). These design points correspond to the designs that have an equivalent short period damping ζ_{sp} above the requirement in the CAP specification.

All designs meet the ADS-33E Level 1 flight path response to pitch attitude requirement (First Tier specification). Like the pitch attitude bandwidth requirement, the MIL-STD-1797B requirement on flight path bandwidth is more stringent than the ADS-33E requirement.

Finally, the dropback requirement is shown in the last subplot in Figure 12 and is met for all designs. As expected, there is near zero dropback for the pitch rate command/attitude hold (RCAH) designs ($V < 200$ kts). There is > 0 dropback for the normal acceleration designs ($V > 200$ kts), although it is well below the maximum allowable value.

Configuration Specific Considerations

Coaxial-Pusher Several configuration-specific modifications were made to the coaxial-pusher control laws. The first modification was inclusion of feed-forward compensation for rotor tip clearance to ensure sufficient separation between the upper and lower rotors during maneuvering flight. As explained in Ref. 3, a rotor tip separation output was included in the coaxial-pusher model. This was done by using the flapping states of each rotor to determine the position of each rotor's tip path plane (TPP) and determining the minimum separation of the two TPPs around the rotor azimuth.

It was noticed early in the coaxial-pusher control law design process, that without compensation for tip clearance, large maneuvers could cause the two rotors to hit (i.e., tip separation < 0). Figure 13 shows a time history of a roll

piloted pulse response at an airspeed of $V = 240$ kts without compensation for rotor tip clearance (blue line). Note that for this roll maneuver, a maximum roll rate of $p \approx 50$ deg/sec is generated, which is about half of the required maximum roll rate specification in ADS-33E for Target Acquisition & Tracking ($p \geq 90$ deg/sec). Even for this reduced roll rate, without the tip clearance controller, the tip path planes of the upper and lower rotors intersect.

To compensate for this, ideal crossfeeds between roll and pitch rate (p and q) and differential lateral and longitudinal cyclic commands ($\Delta\theta'_{1c}$ and $\Delta\theta'_{1s}$) were determined from the differential flapping equations:

$$\begin{bmatrix} \Delta\ddot{\beta}'_{1c} \\ \Delta\ddot{\beta}'_{1s} \end{bmatrix} = \begin{bmatrix} Mf_p & Mf_q \\ Lf_p & Lf_q \end{bmatrix} \begin{bmatrix} p \\ q \end{bmatrix} + \dots \quad (12)$$

$$+ \begin{bmatrix} Mf_{\Delta\theta'_{1c}} & Mf_{\Delta\theta'_{1s}} \\ Lf_{\Delta\theta'_{1c}} & Lf_{\Delta\theta'_{1s}} \end{bmatrix} \begin{bmatrix} \Delta\theta'_{1c} \\ \Delta\theta'_{1s} \end{bmatrix}$$

To not impact the stability characteristics of the control system, the ideal crossfeeds to get $\Delta\ddot{\beta}'_{1c} = \Delta\ddot{\beta}'_{1s} = 0$ are determined using the *commanded* roll and pitch rates (p_{cmd} , q_{cmd}) as:

$$\begin{bmatrix} \Delta\theta'_{1c} \\ \Delta\theta'_{1s} \end{bmatrix} = - \begin{bmatrix} Mf_{\Delta\theta'_{1c}} & Mf_{\Delta\theta'_{1s}} \\ Lf_{\Delta\theta'_{1c}} & Lf_{\Delta\theta'_{1s}} \end{bmatrix}^{-1} \times \quad (13)$$

$$\begin{bmatrix} Mf_p & Mf_q \\ Lf_p & Lf_q \end{bmatrix} \begin{bmatrix} p_{cmd} \\ q_{cmd} \end{bmatrix}$$

Thus, the tip clearance controller is implemented as a feed-forward crossfeed. The underlined terms in Eq. 13 are dominant, and so a simplified on-axis tip clearance feed-forward crossfeed is used:

$$\Delta\theta'_{1c} = - \frac{Lf_q}{Lf_{\Delta\theta'_{1c}}} q_{cmd} \quad (14)$$

$$\Delta\theta'_{1s} = - \frac{Mf_p}{Mf_{\Delta\theta'_{1s}}} p_{cmd}$$

The differential cyclic commands are converted to upper and lower rotor actuator commands which are then summed with the individual actuator commands output by the control allocation section of the control system.

Figure 13 shows a history of the same roll maneuver previously discussed with compensation for rotor tip clearance (dashed, red line). With the tip clearance controller, sufficient separation between the upper and lower rotors is maintained with negligible effects on the roll rate response. Figure 13 also shows the off-axis pitch rate q

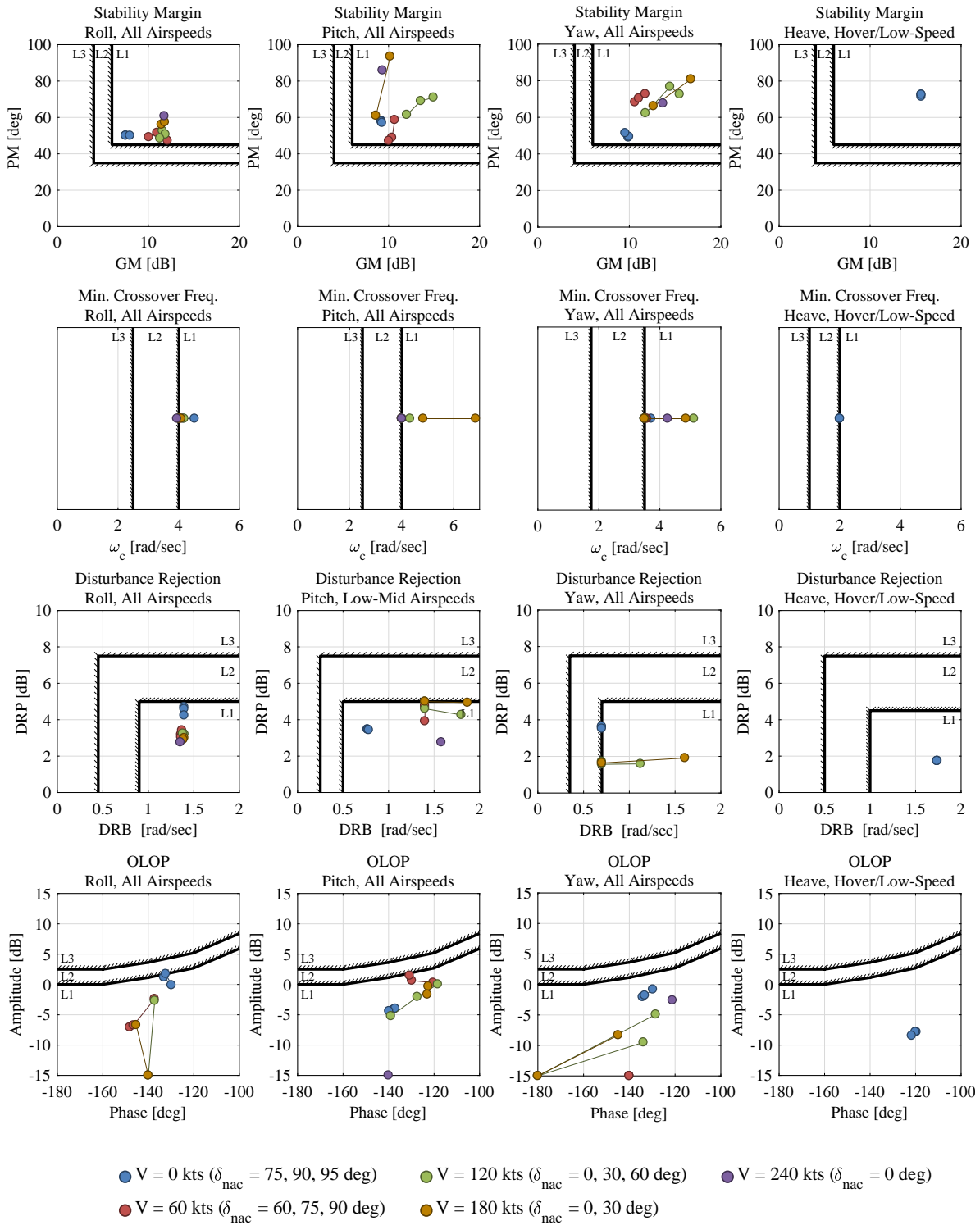


Fig. 11. Example control system design specification and optimized design results (1/2, Tiltrotor, hover–240 kts).

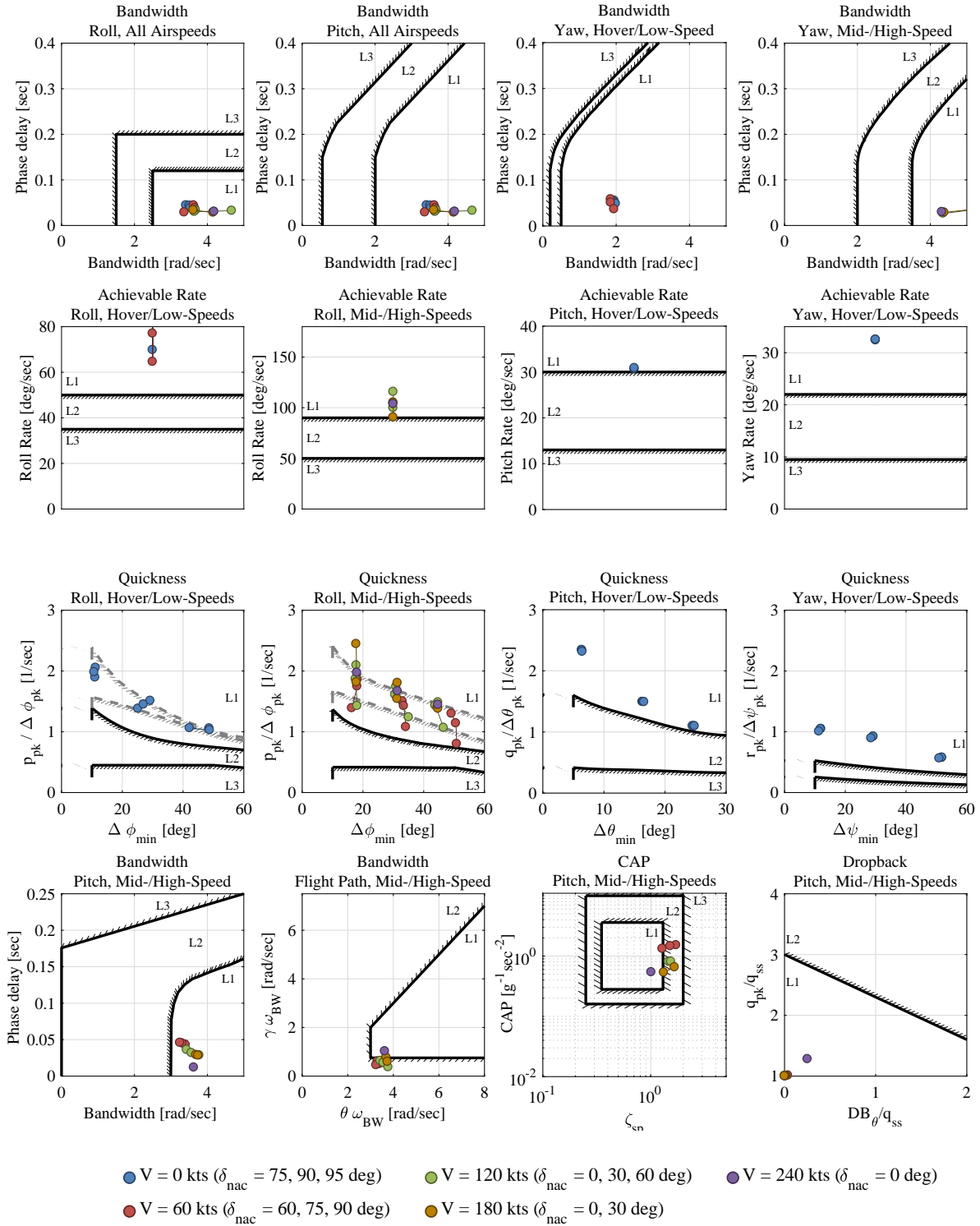


Fig. 12. Example control system design specification and optimized design results (2/2, Tiltrotor, hover–240 kts).

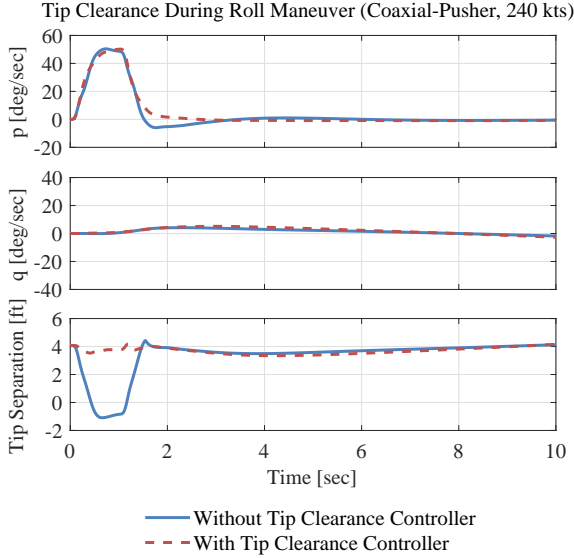


Fig. 13. Tip clearance during roll maneuver (coaxial-pusher, 240 kts).

response during this maneuver which is small and not affected by the tip clearance controller. Similar results are seen in pitch, although since the maximum achievable rate requirements for roll are nearly twice as high as for pitch, the roll axis is more critical.

Note that since the tip clearance controller is implemented in the feed-forward based on commanded roll and pitch rates, instead of in the feedback based on actual roll and pitch rates, large uncommanded aircraft rates may still be an issue. An investigation into tip separation in gusts and turbulence is still needed.

The second configuration-specific modification made to the coaxial-pusher control laws was the inclusion of the a collective trim map on the collective/thrust control lever (TCL). This was done to reduce pilot workload during high-speed flight and acceleration/deceleration maneuvers. The collective trim map is only active above $V = 40$ kts where the vertical axis is open-loop (direct stick to head, Table 1). Figure 14 shows the collective trim map used in the coaxial-pusher control laws. These values correspond to the collective θ_0 values required to trim the aircraft at each airspeed with ship level pitch attitude ($\theta = 0$ deg).

The third configuration-specific modification made to the coaxial-pusher control laws was a set of pilot controls for the pusher propeller. The pusher propeller is controlled via a thumb wheel on the TCL. The wheel commands a pusher propeller collective rate $\dot{\theta}_{0pp}$ proportional to its deflection, with maximum deflection commanding $\dot{\theta}_{0pp} = 7$ deg/sec and forward wheel deflection commanding increased θ_{0pp} (faster airspeed). Once released, θ_{0pp} remains fixed.

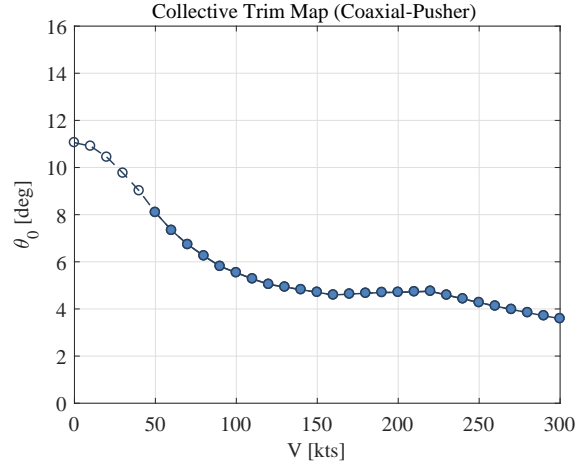


Fig. 14. Collective trim map (coaxial-pusher).

In addition to this thumb wheel, two push buttons can also be used to change pusher propeller collective. The first push button is the Zero Thrust switch and commands the pusher propeller to its zero thrust setting, thus allowing the pilot a way to perform a quick deceleration. The second push button is the Thrust to Airspeed Couple button. This button sets the pusher propeller collective to roughly match the value required to hold the current airspeed with ship level pitch attitude. Note that this is not an airspeed hold mode as there is no airspeed feedback, and is simply a pusher propeller versus airspeed trim map. This button is useful when accelerating/decelerating like a conventional helicopter (with pitch attitude) to a given airspeed and then wanting to re-reference the pitch attitude to $\theta = 0$ deg.

Finally, to manage power, the control laws prioritize the main rotors over the pusher propeller. Therefore, if the pilot were to enter an aircraft state where power required P_{req} exceeded power available P_{avail} , the pusher propeller collective will be reduced until $P_{req} \leq P_{avail}$.

Tiltrotor The tiltrotor-specific modifications include a collective bias map implemented as a function of nacelle angle. This is needed because the tiltrotor has a very large collective trim θ_0 range throughout its flight envelope (Ref. 3), which is beyond the range of the rotor actuators (Table 4). Figure 15 shows the collective trim range for airspeeds spanning the conversion corridor at several nacelle angles, as well as the collective bias map implemented in the control laws which is used to drive the collective trim actuator on each rotor and offload the rotor actuators.

The second configuration-specific modification made to the tiltrotor control laws was a set of pilot controls to command nacelle angle. Nacelle angle δ_{nac} is controlled via a thumb wheel on the TCL. The wheel commands a

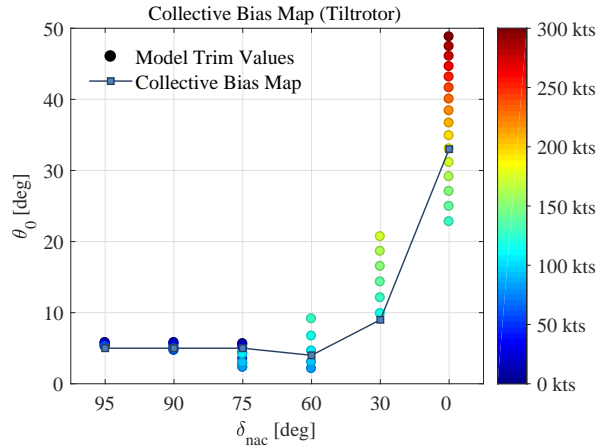


Fig. 15. Collective bias map (tiltrotor).

nacelle angle rate $\dot{\delta}_{nac}$ proportional to its deflection, with forward deflection commanding forward nacelle (down towards airplane mode). The maximum rate is $\dot{\delta}_{nac} = 8$ deg/sec. In addition to the thumb wheel, two push buttons can also be used to cycle the nacelles between preset angles $\delta_{nac} = 0, 30, 60, 75, 90, 95$ deg.

EXPERIMENTAL SETUP

Simulation Facilities

The handling qualities experiment was conducted in the Vertical Motion Simulator (VMS) at NASA Ames Research Center, shown in Figure 16(a). The VMS provides 6-degree of freedom motion with 60 feet of vertical and 40 feet of lateral travel.

Figure 16(b) shows the inside of the Transport Cab (T-Cab) used for this experiment. The cab provides a 180-degree field of view to the pilot (right seat), as well as a chin window. The inceptor configuration consisted of a side-stick attached to the right-hand side by the pilot seat, standard pedals, and a thrust controller lever (TCL) using pull-for-power logic. The TCL had a thumb wheel to control the coaxial-pusher propeller and the tiltrotor nacelle angle, in addition to two special function push buttons for each platform. A heads-up display, depicted on the external world view, kept the pilot focused outside flying rather than on the instrumentation.

Nonlinear Simulation Model Validation

Before beginning handling qualities evaluations, implementation of models in the simulator was validated. This was done by conducting both closed-loop and broken-loop automated frequency sweeps of the nonlinear simulation models. The frequency sweep simulation data were analyzed using CIFER[®] (Ref. 23) to extract the appropriate frequency responses and compare to those of the



(a) Cab external view



(b) Cab internal view

Fig. 16. NASA Ames Vertical Motion Simulator.

linear point model used in the control law development. Three responses were analyzed in each axis: the closed-loop piloted response comparison validates the implementation of the feed-forward and feedback sections of the control laws; the closed-loop disturbance response and broken-loop response comparisons validate the implementation of the stitched model and the feedback section of the control laws.

Figure 17 shows the lateral axis broken-loop frequency responses for both the nonlinear simulation model and linear analysis models of the coaxial-pusher at $V = 180$ kts. There is an excellent agreement between the nonlinear simulation and linear models, validating the implementation of the stitched model, gain schedule, and control laws in the simulation model.

Figure 18 shows a closed-loop lateral pulse response time history comparisons between the nonlinear simulation and linear analysis models of the coaxial-pusher at $V = 180$ kts. The time histories match very well, show-

ing further validation of the nonlinear simulation model used for handling qualities assessment.

Similar comparisons were done for the other axes and at additional airspeeds for the coaxial-pusher and tiltrotor simulation models. All validations showed excellent agreement with the analysis models.

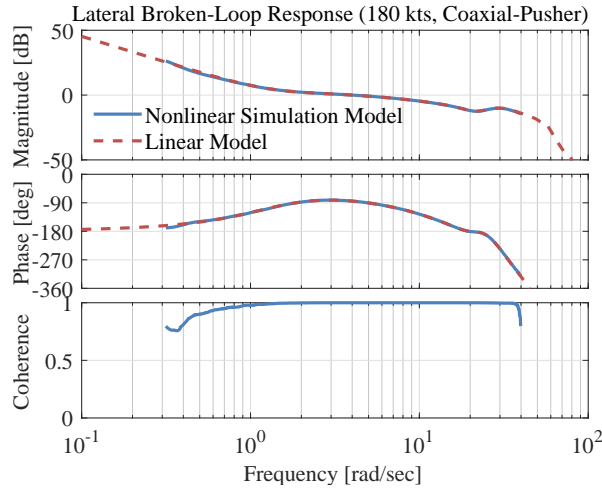


Fig. 17. Lateral broken-loop response comparison (coaxial-pusher, 180 kts).

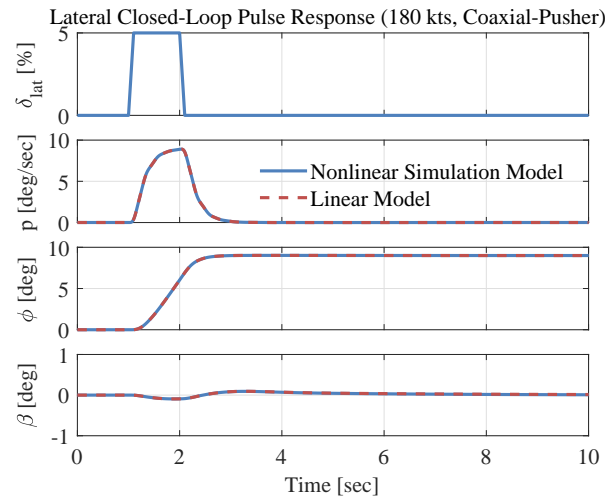


Fig. 18. Lateral closed-loop pulse response comparison (coaxial-pusher, 180 kts).

Handling Qualities Task Definitions

Four newly developed NRTC high-speed MTEs were used to assess the handling qualities of the coaxial-pusher and tiltrotor control laws in the transition and high-speed flight regime. The tasks used are Pitch and Bank Attitude Capture and Hold (Ref. 7), Pitch and Roll Sum-of-Sines

Tracking (Ref. 8), Break Turn (Ref. 9) and High-Speed Acceleration/Deceleration (Ref. 10). The tasks are described in detail in the Appendix, including tables of desired and adequate performance bounds.

Pitch angle capture (PACH) and pitch tracking (Pitch SOS) tasks were flown at two airspeeds ($V = 180$ and 220 kts) to test both longitudinal responses types (RCAH and n_z command). Bank angle capture (BACH), roll tracking (Roll SOS), and the Break Turn maneuver were tested at $V = 180$ kts only. A speed range of $V = 50 - 220$ kts was used for the High-Speed Acceleration/Deceleration.

COAXIAL-PUSHER HANDLING QUALITIES RESULTS

Figure 19 shows the handling qualities ratings (HQRs) collected for the coaxial-pusher aircraft for the high-speed MTEs. The errorbars represent average, maximum, and minimum ratings collected. Average ratings for all MTEs except for the Break Turn are Level 1. The following sections will discuss the results for each MTE in more detail.

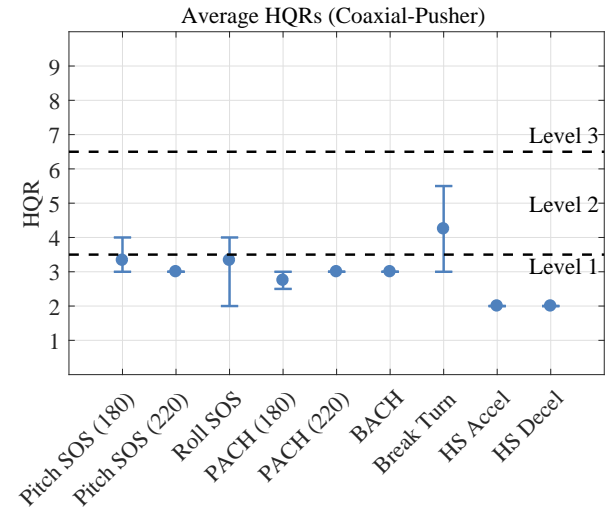


Fig. 19. Handling qualities rating summary (coaxial-pusher).

Pitch Angle Capture and Hold

The Pitch Angle Capture and Hold (PACH) MTE was flown by two pilots (B and D), at two different airspeeds each ($V = 180$ kts and 220 kts). At $V = 180$ kts, the response type in the pitch axis is pitch rate q command, while at $V = 200$ kts, the response type is normal acceleration n_z command.

Pilots met desired performance for all runs. Figure 20 shows one example run for Pilot B at $V = 220$ kts. The

figure shows the target pitch attitude with desired and adequate bounds, and actual aircraft pitch attitude, which remains well within the desired bounds for the entire run.

At $V = 180$ kts, pilots gave the task an average HQR 2.8 and noted that they were “able to meet desired [performance] easily” and be “quite precise,” and that the ride quality was “smooth.”

At $V = 220$ kts, pilots gave an average HQR 3 and had similar comments. One of the pilots noted that the normal acceleration command control laws were “not as tight” as the rate command control laws but that he was not working hard. The pilot also noted a slight tendency to overshoot, but that he was consistently meeting desired and that ride quality was smooth.

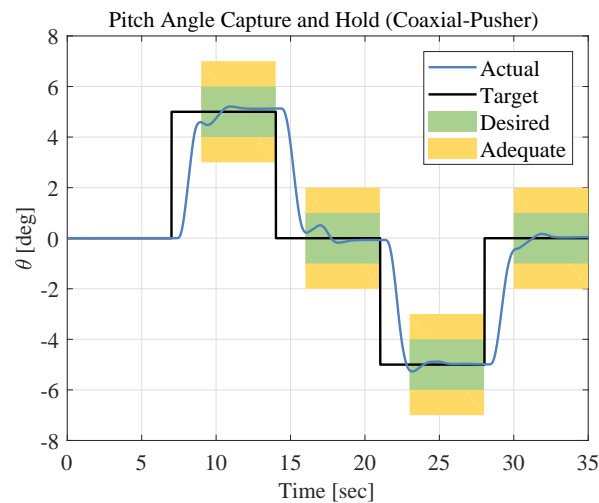


Fig. 20. Pitch Angle Capture and Hold example time history (coaxial-pusher, 220 kts).

Bank Angle Capture and Hold

The Bank Angle Capture and Hold (BACH) MTE was flown by two pilots (B and D) at one airspeed ($V = 180$ kts), since there is no switch in roll response type with airspeed. In all cases, pilots were able to meet desired performance. Figure 21 shows an example run, with the bank angle within desired performance throughout the task.

The two pilots rated this MTE and average HQR 3. Pilot B commented that he was able to meet desired and that the “hold part was easy.” Pilot D commented that he was “consistently able to meet desired” and that the response was “tight.” Pilot D did note that he was inadvertently putting in off-axis inputs when applying large roll inputs, although this did not degrade the performance.

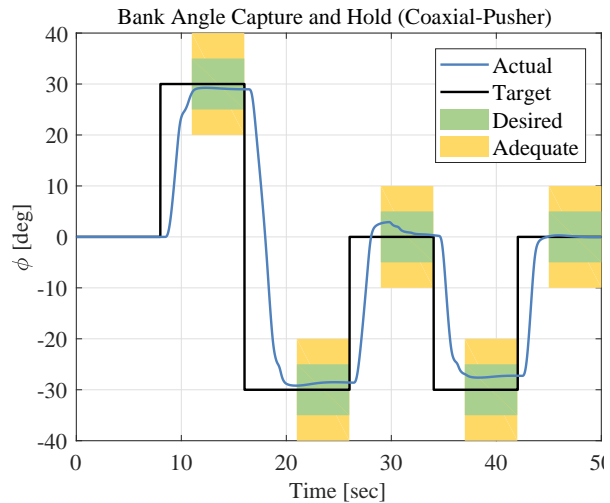


Fig. 21. Bank Angle Capture and Hold example time history (coaxial-pusher, 180 kts).

Pitch Sum-of-Sines Tracking

The Pitch Sum-of-Sines (SOS) Tracking MTE was flown by four pilots. Two of the pilot flew the MTE at $V = 180$ kts (pitch rate q command), one pilot at $V = 220$ kts (normal acceleration n_z command), and one pilot at both airspeeds. Figure 22 shows the tracking performance for the task. All pilots were able to meet desired performance (i.e., percent within desired $\geq 50\%$) by a large margin.

Flying the task at $V = 180$ kts, pilots rated the task an average HQR 3.3 and commented that meeting desired was easy and that the attitude hold made maintenance easy. However, pilots also commented that the response was “heavily/too damped” which required “large inputs to overcome.” The comments about damping are consistent with the values of equivalent short period damping $\zeta_{sp} > 1$ for the $V = 180$ kts design in the CAP specification in Figure 8 (last row, third subplot).

Flying the task at $V = 220$ kts, pilots rated the task an average HQR 3 and commented that they could consistently meet desired performance. Pilots did note that the response at $V = 220$ kts was more “jerky than RCAH” and that the biggest difference between the two airspeeds and response types was in ride quality, which was better at the lower airspeed. However, pilots still noted that there was minimal compensation.

The difference in ride quality between performing the Pitch Sum-of-Sines Tracking task at $V = 180$ kts versus $V = 220$ kts is expected, since the target signal RMS value is the same, requiring the pilot to generate the same pitch rates to meet desired performance at either airspeed. However, the resulting normal acceleration for the same pitch rate is 20% higher at $V = 220$ kts than at $V = 180$ kts. This 20% increase is consistent with the difference

between peak-to-peak normal acceleration values seen in the data for this task at the two airspeeds.

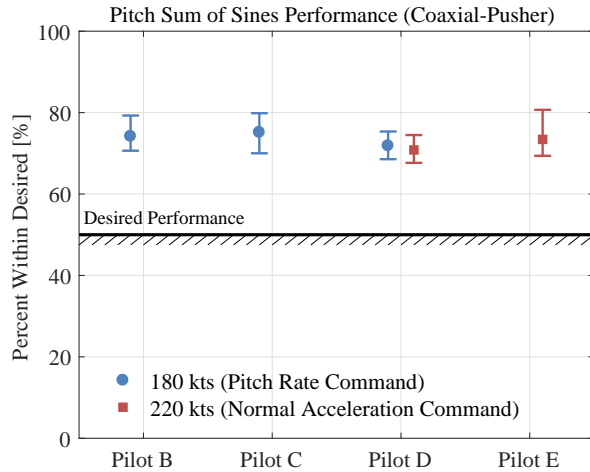


Fig. 22. Pitch Sum-of-Sines Tracking performance (coaxial-pusher).

Roll Sum-of-Sines Tracking

The Roll SOS Tracking MTE was flown by three pilots (B, C, and D) at $V = 180$ kts. Figure 23 shows the tracking performance for the task. All pilots were able to meet desired performance (i.e., percent within desired $\geq 50\%$), although Pilot B did have one run that was just outside of desired performance, but did meet adequate performance. Overall, pilots rated the task an average HQR 3.3 and commented that they could meet desired performance, but with large control inputs to get the necessary angles.

Pilot B did comment that he was “dealing with lots of pitch during roll,” however this was not noted or commented on by the other two pilots. Looking at the data from all the pilots’ runs, it was noted that the aircraft pitch rate q tracked the commanded pitch rate q_{cmd} very closely. The mean RMS error between commanded and actual pitch rate during all runs was $RMS_{q_{err}} = 0.24$ deg/sec. However, it was noted that Pilot B’s longitudinal stick RMS was twice as large as the other two pilots’. This suggest that perhaps the pitch-roll cross-coupling issue that Pilot B noted was actually due to cross contamination of his stick motion, similarly to what Pilot D noted for the BACH task.

Break Turn

The Break Turn MTE was flown by two pilots (A and E). Figure 24 shows the performance for all data runs for both pilots, plotted against the desired and adequate

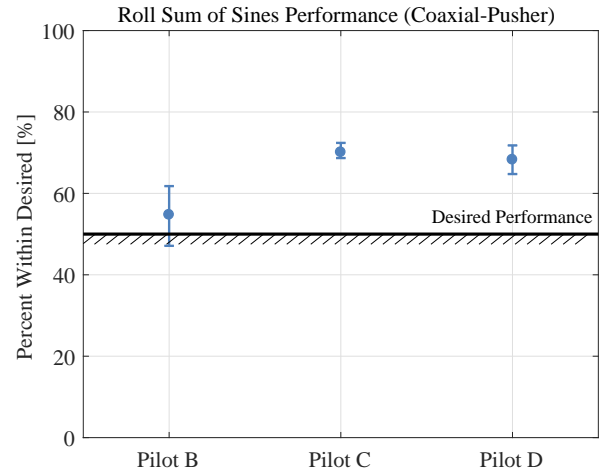


Fig. 23. Roll Sum-of-Sines Tracking performance (coaxial-pusher).

bounds listed in Table 9. Figure 25 shows the pilot stick activity (cutoff frequency ω_{co} and RMS) for all axes during the Break Turn maneuver. The errorbars represent the average, maximum, and minimum values for all of a given pilot’s runs. For axes with 0 RMS, ω_{co} was not calculated. The cutoff frequency ω_{co} is defined as the half-power frequency of the pilot stick signal determined via spectral analysis, and is a measure of the pilot’s operating frequency (Ref. 23).

Pilot A was able to meet desired performance on all parameters except time to complete, which was over the desired time T_{des} by an average of 1.0 sec (Figure 24). Pilot A rated the maneuver an HQR 5.5 and commented that “targeting roll attitude [was] fairly easy” but that “pitch maintenance [was] difficult.” In fact, Pilot A noted that “pitch management during the turn and roll-out” was the critical subphase of this task. These comments correspond to Pilot A’s higher ω_{co} in the longitudinal axis than lateral axis. However, Pilot A was able to maintain both altitude and airspeed within the desired bounds. Pilot A also commented that turn coordination worked well and that he was able to complete the maneuver with his feet on the floor (i.e., no pedal input), which can be seen as the $RMS = 0$ for pedals in Figure 25.

Pilot E rated this MTE an HQR 3 and commented that “aggressiveness was required” to complete the MTE in the desired time, and “precision was there” to stay within the desired bounds. Pilot E also noted that his feet were on the floor throughout the maneuver (pedal $RMS = 0$, Figure 25), and he relied on the control system to provide turn coordination. Pilot E did increase speed using the pusher propeller before entering the turn, as can be seen by the increasing airspeed in the third subplot in Figure 24.

Neither pilot used the TCL during this maneuver (TCL

RMS = 0, Figure 25), preferring to adjust the airspeed by using the pusher propeller thrust control.

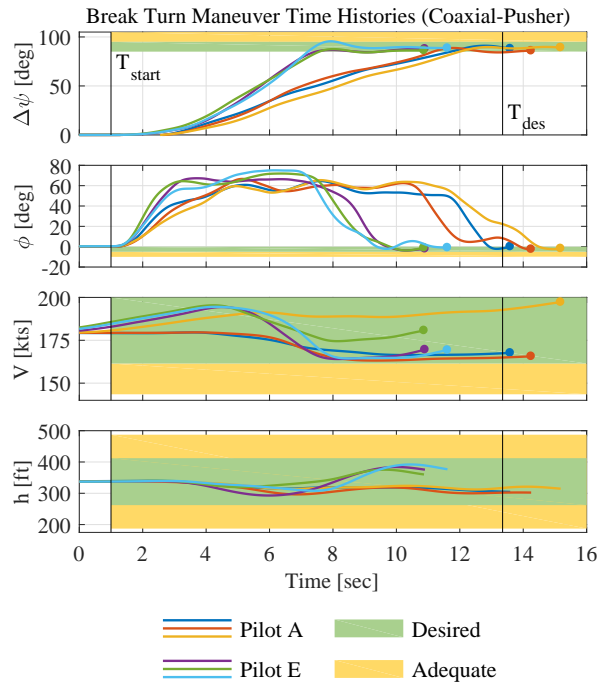


Fig. 24. Break Turn task performance (coaxial-pusher).

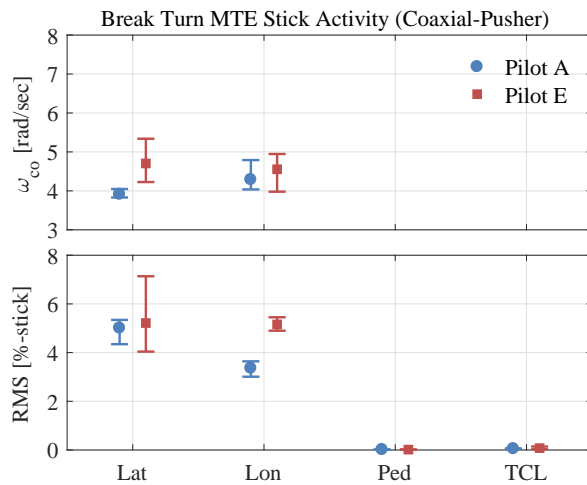


Fig. 25. Break Turn stick activity (coaxial-pusher).

High-Speed Acceleration/Deceleration

Two pilots (A and E) flew the High-Speed Acceleration/Deceleration maneuver with the coaxial-pusher. Figure 26 shows time histories for all record runs for Pilots A and E for the acceleration portion of the maneuver. Both

pilots were able to meet desired performance on all parameters.

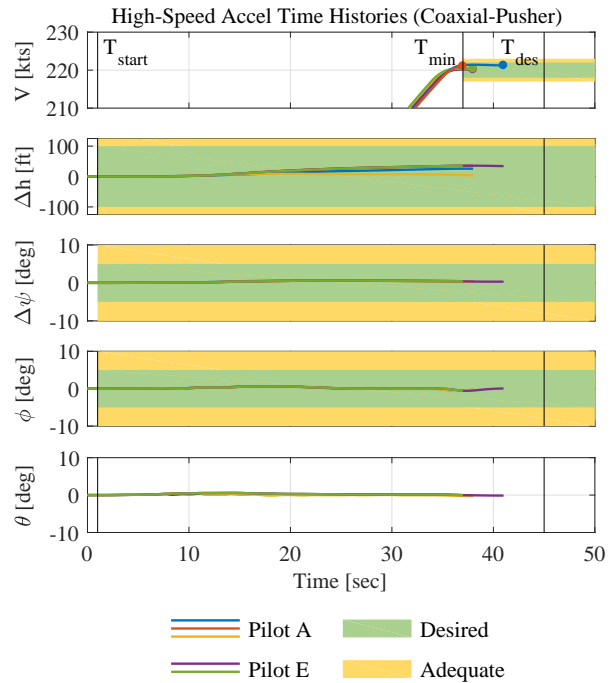


Fig. 26. High-Speed Acceleration task performance (coaxial-pusher).

Pilot A rated the maneuver an HQR 2 and commented that the ability to meet desired was “all but effortless.” His technique was to accelerate by setting the pusher propeller commanded thrust to 100% and then use the Thrust to Airspeed Couple button at $V = 217$ kts to capture $V = 220$ kts. Pilot A also noted that the maneuver required no inputs on the lateral stick or pedals.

Pilot E rated the maneuver an HQR 2 and commented that he used the link to airspeed button to manage speed, which was “very precise.” Pilot E noted some slight climbs, but that they were easily adjusted, and noted that the maneuver required very little compensation.

Figure 26 also shows the pitch attitude θ during the acceleration maneuver. Neither pilot had to adjust pitch attitude throughout the maneuver, since the coaxial-pusher can trim at $\theta = 0$ deg at all airspeeds. The collective trim map for the coaxial-pusher enabled the pilots to maintain altitude well within desired performance while performing a high-rate acceleration with inputs on the longitudinal stick and TCL of $< 0.5\%$ RMS, as shown in Figure 27. Note that pilot cutoff frequency ω_{co} was not calculated for cases of 0 RMS.

Figure 28 shows time histories for all record runs for Pilots A and E for the deceleration portion of the maneuver. Both pilots were able to meet desired performance on all

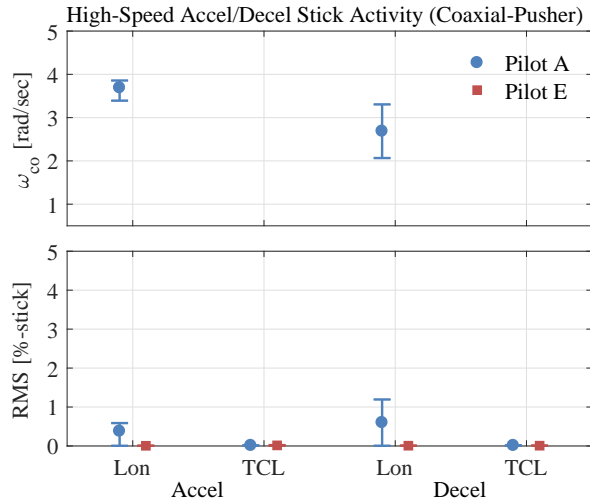


Fig. 27. High-Speed Acceleration/Deceleration stick activity (coaxial-pusher).

parameters and rated the deceleration portion of the maneuver an HQR 2. Both pilots noted that they were able to meet desired performance using the pusher propeller thumbwheel and button controls only, with hands off all the other controls, which corresponds to the stick activity data for deceleration shown in Figure 27. In addition, as with the acceleration portion, pilots did not need to adjust the aircraft pitch attitude to control airspeed or altitude while transitioning through a wide range of airspeeds.

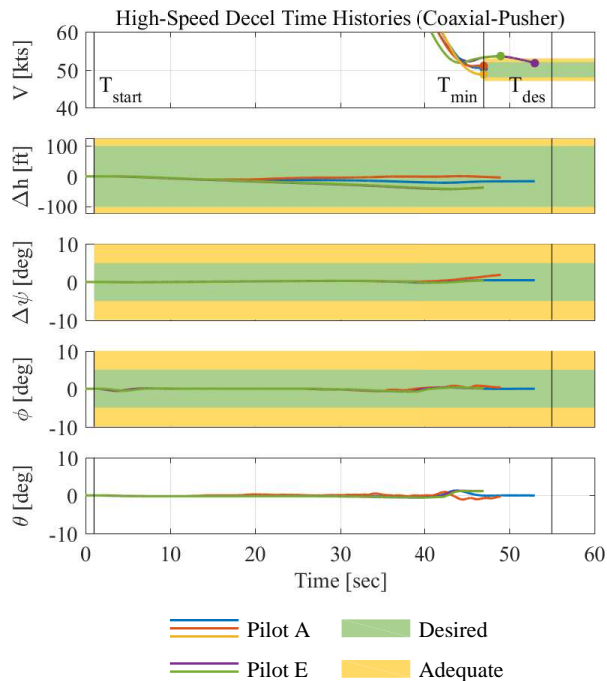


Fig. 28. High-Speed Deceleration task performance (coaxial-pusher).

TILTROTOR HANDLING QUALITIES RESULTS

Figure 29 shows the handling qualities ratings (HQRs) collected for the tiltrotor aircraft for the high-speed MTEs. The errorbars represent average, maximum, and minimum ratings collected. Average ratings for all MTEs except for the High-Speed Acceleration/Deceleration are Level 1. The following sections will discuss the results for each MTE in more detail.

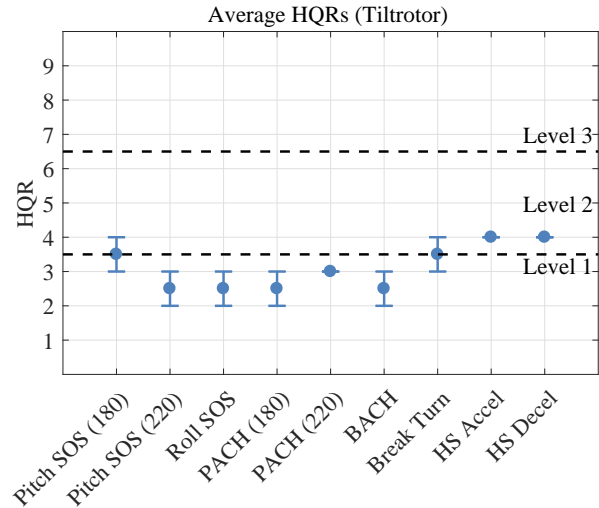


Fig. 29. Handling qualities rating summary (tiltrotor).

Pitch Angle Capture and Hold

The Pitch Angle Capture and Hold MTE was flown by two pilots, at two different airspeeds each ($V = 180$ kts and 220 kts). At $V = 180$ kts, the response type in the pitch axis is pitch rate q command, while at $V = 220$ kts, the response type is normal acceleration n_z command.

Pilots met desired performance in all runs. Figure 30 shows one example run for Pilot B at $V = 180$ kts. The figure shows the target pitch attitude with desired and adequate bounds, and actual aircraft pitch attitude, which remains inside the desired bounds for the entire run.

At $V = 180$ kts, pilots gave the task an average HQR 2.5 and commented that it was “easy to meet desired [performance]” and “very easy to point the nose.” They also noted that the response was “very precise” and they were able to use one single input.

At $V = 220$ kts, pilots gave the task an average HQR 3. Pilot B commented that he was able to meet desired performance, but that he was getting “slightly larger errors compared to 180 kts,” with some overshoots and “pitch bobbles.” Pilot A commented that he could also make desired, but precision was less compared to $V = 180$ kts,

Roll Sum-of-Sines Tracking

The Roll Sum-of-Sines Tracking MTE was flown by two pilots (B and C) at $V = 180$ kts. Figure 33 shows the task performance for each pilot's runs. Both pilots were able to meet desired performance for all runs and rated this task an average HQR 2.5.

Both pilots noted that the pitch axis was a factor during this roll tracking task. However, inspection of the pitch rate data showed that it matched the commanded pitch rate with average RMS error less than 0.1 deg/sec. In addition, all designs meet the Level 1 ADS-33E pitch-due-to-roll coupling requirement for Target Acquisition & Tracking. This suggests that either the pilots were inadvertently commanding pitch during the maneuver or that pitch turn compensation was a factor for this task. It is notable that for the more discrete roll inputs used in the bank angle capture and hold tasks, pilots commented that pitch never left the desired circle.

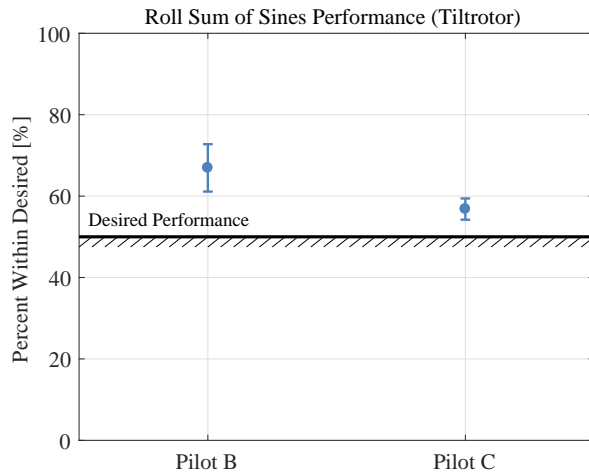


Fig. 33. Roll Sum-of-Sines Tracking performance (tiltrotor).

Break Turn

The Break Turn MTE was flown by two pilots (A and E). Figure 34 shows the performance for all data runs for both pilots, plotted against the desired and adequate bounds listed in Table 9. Both pilots were able to meet desired performance on all parameters.

Pilot A rated the maneuver and HQR 3 and commented that it was “easy to target bank angle” and that no pedal inputs were required to coordinate the turn. Pilot A noted that he was putting a step input on the thrust control lever one second before starting the turn, which is evident by the increase in airspeed in Pilot A's runs in Figure 34.

Pilot E rated this MTE an HQR 4, although he used a different control strategy than Pilot A. Pilot E noted that he decreased airspeed going into the turn in order to increase turn rate. This led to Pilot E having slightly shorter time to complete the maneuver than Pilot A, as seen by Pilot E's runs in Figure 34. Even though the airspeed dropped below desired performance during Pilot E's runs, he was able to bring airspeed back into desired at the end of the turn and therefore meet desired performance.

Figure 35 shows the pilot stick activity (cutoff frequency ω_{co} and RMS) for both the lateral and longitudinal axes during the Break Turn maneuver. Both pilots have similar stick activity in the lateral and longitudinal axes, and in Pilot E's case in the TCL axis suggesting that although this is primarily a roll task, speed and altitude management requires comparable pitch inputs. Neither pilot had any activity on the pedals, thus suggesting that turn coordination worked well.

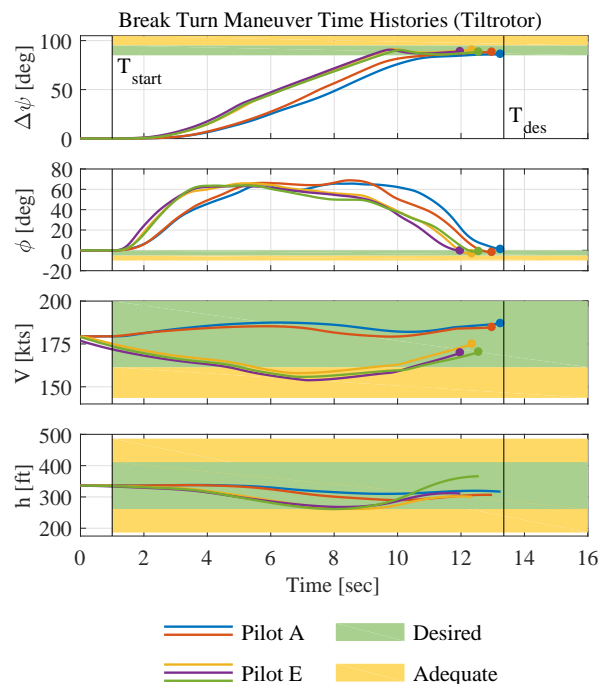


Fig. 34. Break Turn task performance (tiltrotor).

High-Speed Acceleration/Deceleration

Pilot E flew the High-Speed Acceleration/Deceleration maneuver with the tiltrotor. Figure 36 shows time histories for all of Pilot E's record runs for the acceleration portion of the maneuver. Pilot E was able to meet desired performance on all parameters for both of his Acceleration runs. Pilot E rated the Acceleration portion of this MTE an HQR 4 and commented that “aggressiveness

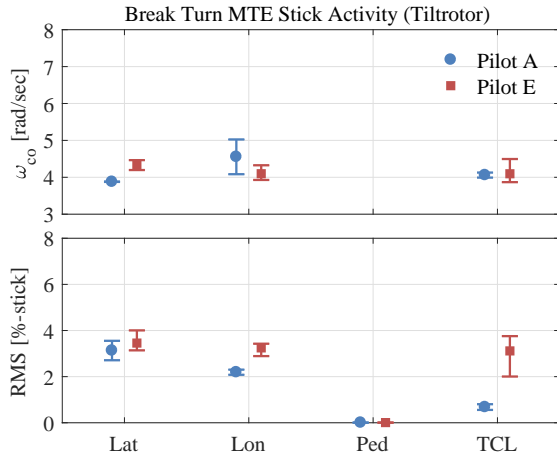


Fig. 35. Break Turn stick activity (tiltrotor).

was required in power and longitudinal to maintain altitude and airspeed.” Pilot E further commented that this was “primarily an altitude maneuver” that required “constant longitudinal control activity.” Figure 36 also shows the tiltrotor pitch attitude θ throughout the acceleration maneuver. Since the tiltrotor transitions from rotor-borne to wing-borne flight during this maneuver, the pilot must trim the aircraft angle of attack α (and therefore pitch attitude θ) as airspeed changes.

Figure 37 shows time histories for all of Pilot E’s record runs for the deceleration portion of the maneuver. Pilot E had an initial run that was beyond the desired time T_{des} but did meet the adequate time requirement. However, his remaining two record runs were all within desired. Pilot E assigned the deceleration portion of the maneuver an HQR 4. He commented that he was “able to meet desired” and be aggressive with the nacelle rates and power inputs. He also noted that he was “focused on height control” and “cross checked [the Vertical Speed Indicator] to meet the altitude tolerance.” Figure 37 also shows pitch attitude θ throughout the deceleration maneuver, and as with the acceleration portion, the pilot had to constantly adjust pitch attitude throughout the maneuver.

Figure 38 shows the pilot longitudinal stick and TCL activity (cutoff frequency ω_{c0} and RMS) during the acceleration and deceleration maneuvers. The pilot had to trim pitch attitude with the longitudinal stick and control airspeed with the TCL throughout the maneuvers, and the resulting average stick RMS was about 3% of stick deflect, with a cutoff frequency $\omega_{c0} \approx 2$ rad/sec.

DISCUSSION

Coaxial-Pusher Tip Clearance Controller

Throughout the handling qualities experiment in the VMS, the coaxial-pusher model logged over four hours of

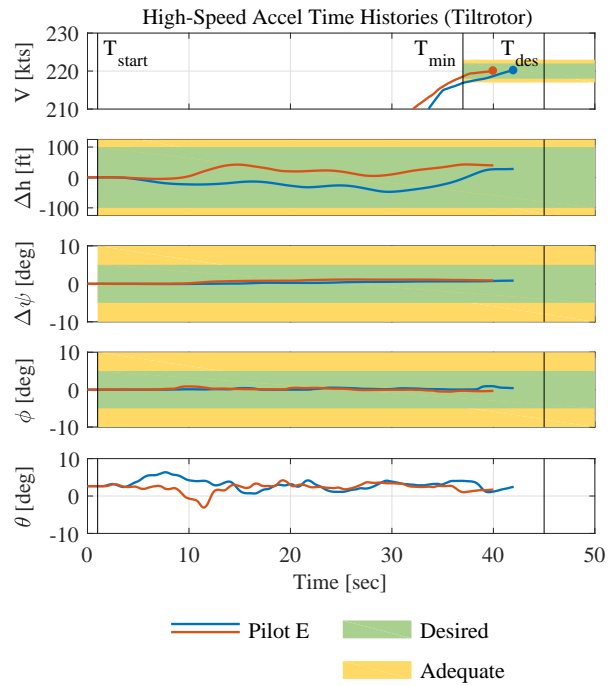


Fig. 36. High-Speed Acceleration task performance (tiltrotor).

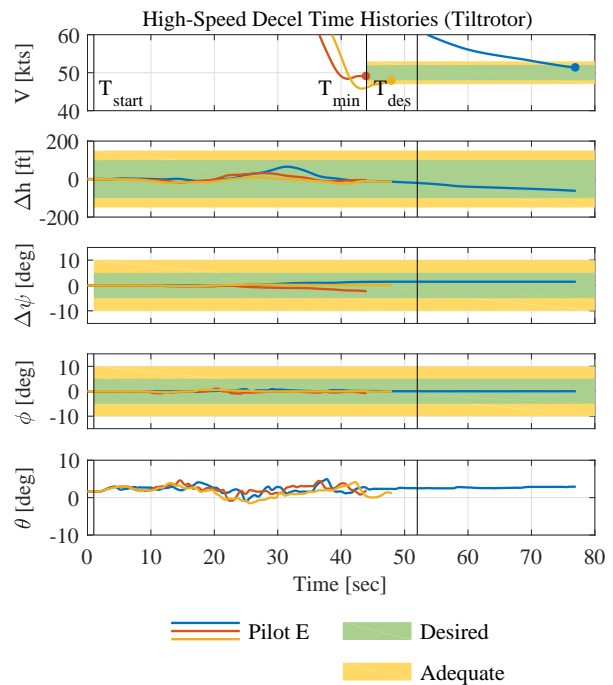


Fig. 37. High-Speed Deceleration task performance (tiltrotor).

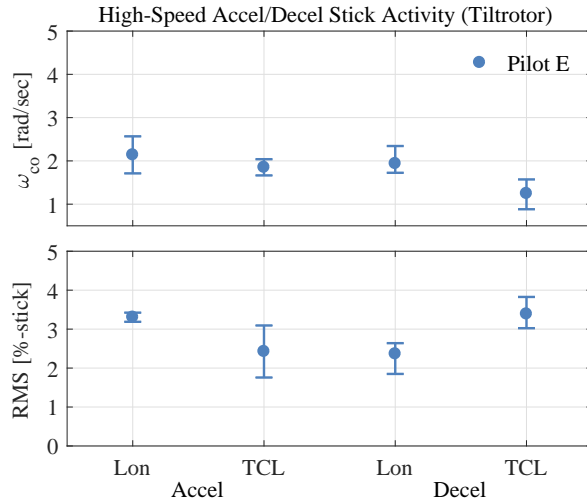


Fig. 38. High-Speed Acceleration/Deceleration stick activity (tiltrotor).

simulation time, during which the minimum rotor separation was 1.2 ft. In a separate VMS simulation experiment using the models and control systems described here, the coaxial-pusher model logged over 20 hours of simulation time, during which the minimum rotor separation was 1.5 ft. This demonstrates the success of the tip clearance feed-forward controller designed for the coaxial-pusher.

MIL-STD-1797B Specifications

Handling qualities specifications from the fixed-wing requirement MIL-STD-1797B worked well to supplement ADS-33E high-speed requirements for both aircraft. In some cases where there is overlap, the MIL-STD-1797B for Category A, Class I requirements are more stringent than the ADS-33E High Agility/Target Acquisition & Tracking requirements, such as for pitch attitude bandwidth and flight path bandwidth/lag.

The lower-order equivalent system specifications from MIL-STD-1797B were applied to both aircraft, when LOES fits had cost functions $J_{LOES} \leq 50$, indicating an excellent match between the lower-order system and high-order aircraft closed-loop response (Ref. 23). For both aircraft, pitch LOES costs were $J_{LOES} < 50$ above $V = 80$ kts and $J_{LOES} < 10$ above $V = 130$ kts, indicating a classical fixed-wing-like response for both RCAH and n_z -command response types. In the roll and yaw axes, $J_{LOES} < 10$ above $V = 80$ kts for both aircraft.

Pitch Rate Command Versus Normal Acceleration Command

The differences in average HQRs for the Pitch Angle Capture and Hold and Pitch Sum-of-Sines Tracking tasks

between the pitch rate command response type and normal acceleration command response types was $\Delta HQR = 0.3$ for the coaxial-pusher and $\Delta HQR = 0.1$ for the tiltrotor. These small difference for both aircraft, shows that both response types work well for the MTEs tested.

For both aircraft, pilots did note during the Pitch Sum-of-Sines Tracking MTE that the pitch response was too heavily damped. This correlates well with the high equivalent short period damping ζ_{sp} seen in the CAP specification, as well as the Level 2 flight path bandwidth values for the RCAH designs. However, since the pitch rate command model is first-order, there is no damping term to tune. A higher-order pitch rate command model, that tracks a classic first-over-second-order pitch rate response, should be investigated.

This result also indicates that the CAP and flight path bandwidth specifications should be First Tier specification in both coax-pusher and tiltrotor designs.

Pitch Stick Contamination During Roll MTEs

For both aircraft, three out of the four pilots that flew the Roll Sum-of-Sines MTE noted pitch excursions/coupling. This issue was not noted for the Bank Angle Capture and Hold MTE, though, which is a task that requires more discrete lateral stick inputs.

One pilot noted that during the Bank Angle Capture and Hold MTE, he inadvertently put in pitch inputs while applying large roll inputs. Since in all cases, the aircraft pitch rates tracked the commanded rates, it appears the coupling issues were caused by stick inputs. It is possible that the pilots did not notice the stick contamination during the continuous tracking of the Sum-of-Sines tasks, unlike the discrete inputs of the Capture and Hold task.

Pilot-Vehicle System Comparison

The control laws for both aircraft use the same architecture and were optimized to meet the same set of specifications. Therefore, it was expected that they would have similar handling qualities ratings, which was the case for tasks that did not require a configuration change (e.g., changing nacelle position in the tiltrotor).

One way to quantitatively compare how pilots flew both aircraft is to investigate the characteristics of the pilot Y_p vehicle Y_c system (PVS) for a given task. In the case of the Sum-of-Sines Tracking tasks, the forcing function of the PVS is known, and so all elements of the PVS can be identified and compared between the two aircraft. Since Pilot C flew the pitch Sum-of-Sines Tracking task using both aircraft and had similar performances (Table 6), his data will be used for this comparison.

Figure 39 shows the PVS broken-loop frequency response ($Y_p Y_c$) extracted from the time history data at the discrete frequencies used in the tracking signal using CIPHER[®]. The figure also shows a crossover model (Ref. 24) fit to the each response. The crossover model is given by:

$$Y_p Y_c = \frac{\omega_c}{s} e^{-\tau s} \quad (15)$$

where:

Y_p denotes the pilot response ($\delta_{stk}/\theta_{err}$),
 Y_c denotes the aircraft response (θ/δ_{stk}),
 ω_c is the crossover frequency, and
 τ is the equivalent time delay.

The parameters of the crossover model are given in Table 6 for both aircraft.

The extracted PVS broken-loop frequency responses of both aircraft match very well, as do the crossover models fit to each response. In fact, as shown in Table 6, the PVS crossover frequency ω_c , which is interpreted as the fundamental frequency of piloted control inputs for closed-loop regulation (Ref. 23), has only a 2% difference between both aircraft. In addition, the PVS crossover models for both aircraft have similar gain margins, phase margins, and time delays.

To further investigate if the pilot was altering his compensation between the two aircraft in order to get a similar PVS response, the individual elements of the PVS were investigated. Figure 40 shows the frequency response of both aircraft Y_c extracted from their respective linear models and from the tracking task data at the discrete frequencies used in the tracking signal. As expected, both aircraft have nearly identical frequency responses, since their control systems use the same command models and were tuned to meet the same set of specifications.

Finally, Figure 41 shows the pilot Y_p frequency response of both aircraft extracted from the tracking task data. In addition, Table 6 lists the parameters of a simple pilot model given by:

$$Y_p = K_p e^{\tau_p s} \quad (16)$$

that was fit to the data for both aircraft. Table 6 also lists the pilot cutoff frequency (ω_{co}) as well as the pilot stick RMS. Based on the pilot frequency responses and pilot model parameters, the pilot behavior between the two aircraft was very similar.

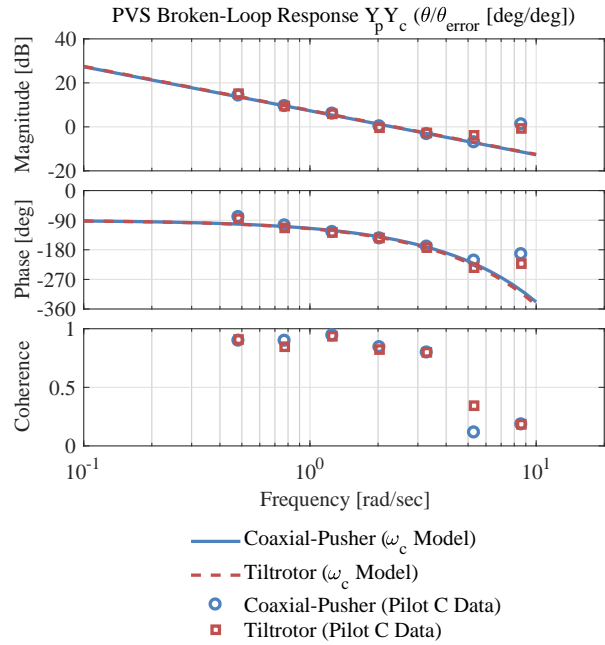


Fig. 39. Pilot-Vehicle System broken-loop frequency responses comparison for Pitch Sum-of-Sines Tracking task (coaxial-pusher and tiltrotor, 180 kts).

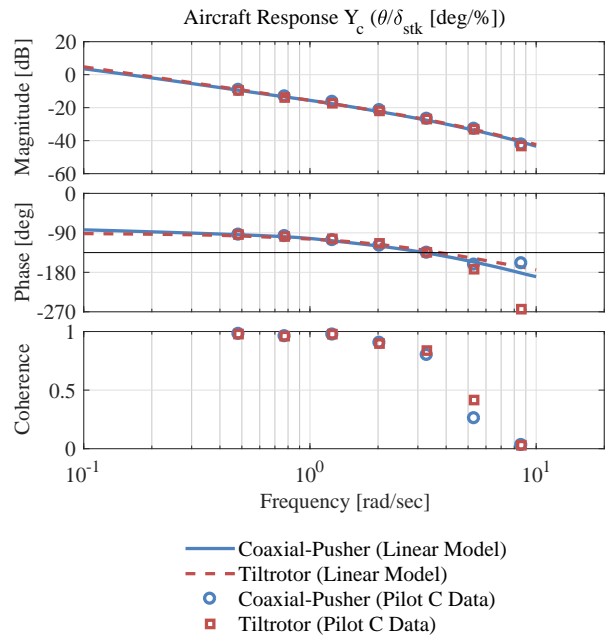


Fig. 40. Vehicle frequency responses comparison for Pitch Sum-of-Sines Tracking task (coaxial-pusher and tiltrotor, 180 kts).

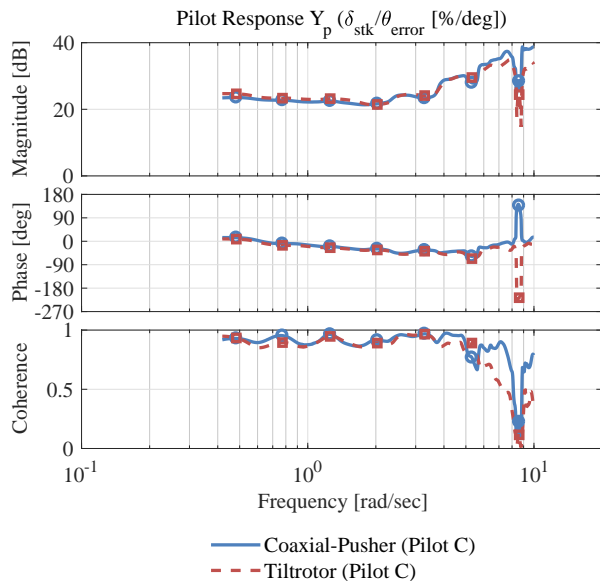


Fig. 41. Pilot frequency responses comparison for Pitch Sum-of-Sines Tracking task (coaxial-pusher and tiltrotor, 180 kts).

Outer Loops

For both aircraft, pilots were asked which outer-loop modes would help improve performance and/or reduce pilot workload for the MTEs. For the coaxial-pusher, pilots answered that airspeed hold would help for the Sum-of-Sines Tracking tasks and altitude hold for the Break Turn MTE. For the tiltrotor, pilots answered that altitude hold would help for the High-Speed Acceleration/Deceleration task. These answers correlate well with high pilot longitudinal stick RMS values for the Break Turn MTE in the coaxial-pusher and high longitudinal stick and TCL RMS values for the tiltrotor during the High-Speed Acceleration/Deceleration task.

High-Speed MTEs

This simulation experiment was the first use of the newly proposed high-speed MTEs in the VMS and by many of the participating pilots. When providing the pilot ratings and comments, pilots were also asked to comment on the appropriateness of the MTEs. In all cases, pilots commented that the MTEs were appropriate for assessing the handling qualities of these aircraft. Pilots commented that the BACH and PACH MTEs were appropriate to see stick characteristics, damping, and bandwidth/phase delay.

Pilots noted that the desired tolerance on the Pitch SOS Tracking MTE was too easy. It would be advisable to use the Precision, Aggressive version of this MTE moving

Table 6. Pilot-Vehicle Parameters for Pitch Sum-of-Sines Tracking Task (180 kts)

	Coaxial-Pusher	Tiltrotor
<i>Pilot-Vehicle System Parameters ($Y_p Y_c$)</i>		
Pilot-Vehicle Crossover Frequency ω_c [rad/sec]	2.32	2.37
Gain Margin [dB]	3.84	3.35
Phase Margin [deg]	32.18	28.80
Pilot-Vehicle Equivalent Time Delay τ [sec]	0.43	0.45
<i>Pilot Parameters (Y_p)</i>		
Pilot Gain K_p	13.50	14.43
Time Delay τ_p [sec]	0.23	0.29
Cutoff Frequency ω_{co} [rad/sec]	1.25	1.23
Stick RMS [%]	11.32	12.23
<i>Performance</i>		
% Within Desired	75.14	79.54

forward, instead of the Precision, Non-Aggressive version used here. Pilots did note that the Roll SOS Tracking MTE seemed reasonable.

For the Break Turn MTE, it was noted that the desired timing tolerance may be too tight, and this MTE received the worst HQR (5.5).

CONCLUSIONS

This paper described the development and handling qualities assessment of flight control systems for a generic lift offset coaxial and a tiltrotor rotorcraft. Overall, both aircraft were assigned Level 1 HQRs in the transition and high-speed flight regimes. The following conclusions are drawn:

1. The explicit model following architecture used for both aircraft worked well throughout their large flight envelopes (hover-300 kts). This architecture made it simple to transition between response types, while maintaining similar performance of the feedback loop (crossover frequency and disturbance rejection bandwidth).
2. The multi-objective optimization method used to tune the control system parameters proved capable of determining designs which concurrently met a large number of frequency- and time-domain specifications while minimizing over-design (i.e., most economical use of actuators and noise sensitivity). Some overlap was identified between the First Tier requirements from ADS-33E and Second Tier requirements from MIL-STD-1797B, and pilot

comments that the pitch RCAH response was too damped correlated well with Second Tier requirements that were not met (CAP and flight path bandwidth). The CAP and flight path bandwidth requirements should be moved to the First Tier for future designs.

3. The tip clearance feed-forward controller for the coaxial-pusher worked well to maintain separation between the upper and lower rotors during all MTEs tested. In addition, the coaxial-pusher collective trim map implementation resulted in very low pilot workload to maintain altitude while accelerating/decelerating through large speed ranges.
4. The Pitch and Bank Angle Capture and Hold, Pitch and Roll Sum-of-Sines Tracking, Break Turn, and High-Speed Acceleration/Deceleration MTEs worked well to assess the high-speed handling qualities of both aircraft tested. Pilots commented that the MTEs were appropriate, but noted that the Precision, Non-Aggressive version of the Pitch Sum-of-Sines Tracking tasks was too easy and that the Break Turn timing tolerance may be too tight.
5. When performing single flight condition tasks, the HQRs and performance between both aircraft were very similar. In addition, pilot control strategy was nearly identical as seen by the Pilot-Vehicle System analysis shown for the Pitch Sum-of-Sines Tracking task.

ACKNOWLEDGMENTS

The authors would like to thank the entire NASA Ames VMS team for making this experiment possible. Furthermore, the authors would like to thank the test pilots that participated in this handling qualities simulation study—MAJ Mark Cleary, LTC Dave Hnyda, MAJ Zach Morford, LTC Carl Ott, and CW3 Tom Wiggins—for providing their time, insight, and excellent comments.

REFERENCES

¹Juhasz, O., Celi, R., Ivler, C. M., Tischler, M. B., and Berger, T., “Flight Dynamic Simulation Modeling of Large Flexible Tiltrotor Aircraft,” American Helicopter Society 68th Annual Forum Proceedings, Fort Worth, TX, May 2012.

²Celi, R., “HeliUM 2 Flight Dynamic Simulation Model: Developments, Technical Concepts, and Applications,” American Helicopter Society 71st Annual Forum, Virginia Beach, VA, May 2015.

³Berger, T., Juhasz, O., Lopez, M. J. S., Tischler, M. B., and Horn, J. F., “Modeling and Control of Lift Offset Coaxial and Tiltrotor Rotorcraft,” 44th European Rotorcraft Forum Proceedings, Delft, The Netherlands, September 2018.

⁴Tischler, M. B., Berger, T., Ivler, C. M., Mansur, M. H., Cheung, K. K., and Soong, J. Y., *Practical Methods for Aircraft and Rotorcraft Flight Control Design: An Optimization-Based Approach*, AIAA, Reston, VA, 2017.

⁵Tobias, E. L. and Tischler, M. B., “A Model Stitching Architecture for Continuous Full Flight-Envelope Simulation of Fixed-Wing Aircraft and Rotorcraft from Discrete-Point Linear Models,” U.S. Army AMRDEC Special Report RDMR-AF-16-01, April 2016.

⁶Tischler, M. B. and Remple, R. K., *Aircraft and Rotorcraft System Identification: Engineering Methods with Flight Test Examples*, AIAA, second edition, Reston, VA, 2012.

⁷Klyde, D. H. *et al.*, “Piloted Simulation Evaluation of Attitude Capture and Hold MTEs for the Assessment of High-Speed Handling Qualities,” AHS International 74th Annual Forum Proceedings, Phoenix, AZ, May 2018.

⁸Klyde, D. H. *et al.*, “Piloted Simulation Evaluation of Tracking MTEs for the Assessment of High-Speed Handling Qualities,” AHS International 74th Annual Forum Proceedings, Phoenix, AZ, May 2018.

⁹Xin, H. *et al.*, “Further Development and Piloted Simulation Evaluation of the Break Turn ADS-33 Mission Task Element,” AHS International 74th Annual Forum Proceedings, Phoenix, AZ, May 2018.

¹⁰Brewer, R. L. *et al.*, “Further Development and Evaluation of a New High-Speed Acceleration / Deceleration ADS-33 Mission Task Element,” AHS International 74th Annual Forum Proceedings, Phoenix, AZ, May 2018.

¹¹Johnson, W., Moodie, A. M., and Yeo, H., “Design and Performance of Lift-Offset Rotorcraft for Short-Haul Missions,” American Helicopter Society Future Vertical Lift Aircraft Design Conference Proceedings, San Francisco, CA, January 2012.

¹²Enns, D., “Control Allocation Approaches,” AIAA Guidance, Navigation and Control Conference, Boston, MA, August 1998.

¹³Ivler, C. M. and Juhasz, O., “Evaluation of Control Allocation Techniques for Medium Lift Tilt-Rotor,” American Helicopter Society 71st Annual Forum Proceedings, Virginia Beach, VA, May 2015.

¹⁴Anon., “Handling Qualities Requirements for Military Rotorcraft,” Aeronautical Design Standard-33 (ADS-33E-PRF), US Army Aviation and Missile Command, March 2000.

¹⁵Berger, T., Tischler, M. B., Hagerott, S. G., Gangsaas, D., and Saeed, N., “Longitudinal Control Law Design and Handling Qualities Optimization for a Business Jet Flight Control System,” AIAA Atmospheric Flight Mechanics Conference Proceedings, Boston, MA, August 2012.

¹⁶Berger, T., Tischler, M. B., Hagerott, S. G., Gangsaas, D., and Saeed, N., “Lateral/Directional Control Law Design and Handling Qualities Optimization for a Business Jet Flight Control System,” AIAA Atmospheric Flight Mechanics Conference Proceedings, Boston, MA, August 2013.

¹⁷Tischler, M. B., “Digital Control of Highly Augmented Combat Rotorcraft,” NASA-TM-88346, May 1987.

¹⁸Anon., “Aerospace - Flight Control Systems - Design, Installation and Test of Piloted Military Aircraft, General Specification For,” SAE-AS94900, July 2007.

¹⁹Berger, T., Ivler, C. M., Berrios, M. G., Tischler, M. B., and Miller, D. G., “Disturbance Rejection Handling Qualities Criteria for Rotorcraft,” AHS International 72nd Annual Forum Proceedings, West Palm Beach, FL, May 2016.

²⁰Duda, H., “Prediction of Pilot-in-the-Loop Oscillations Due to Rate Saturation,” *Journal of Guidance, Navigation, and Control*, Vol. 20, No. 3, May-June 1997.

²¹Lehmann, R., Tischler, M. B., and Blanken, C. L., “Evaluation of ADS-33E Yaw Bandwidth and Attitude Quickness Boundaries,” AHS International 72nd Annual Forum Proceedings, West Palm Beach, FL, May 2016.

²²Anon., “Flying Qualities of Piloted Aircraft,” MIL-STD-1797B, Department of Defense Interface Standard, February 2006.

²³Tischler, M. B. and Remple, R. K., *Aircraft and Rotorcraft System Identification: Engineering Methods and Flight Test Examples Second Edition*, AIAA, 2012.

²⁴McRuer, D. T. and Jex, H. R., “A Review of Quasi-Linear Pilot Models,” *IEEE Transactions on Human Factors in Electronics*, Vol. HFE-8, (3), September 1967, pp. 231–249.

APPENDIX

MISSION TASK ELEMENT PERFORMANCE CRITERIA

Pitch/Bank Angle Capture and Hold

The attitude capture and hold tasks (Ref. 7) are precision, non-aggressive maneuvers. The tasks are flown using the display shown in Figure 42, which is driven by a reference signal composed of a series of step changes in attitude. From steady, wings level flight the aircraft is pitched or banked to capture and maintain the commanded angle within the specified tolerance for 5 sec. Pitch attitudes of ± 5 deg are used and roll attitudes of ± 30 deg are used.

The objective of the task is to evaluate the ability to pitch/bank the aircraft and capture a desired attitude. Additionally, the task identifies maneuverability limitations, inceptor characteristics, cross coupling, and any PIO tendencies.

Table 7 lists the desired and adequate performance criteria for the Bank/Pitch Angle Capture and Hold tasks.

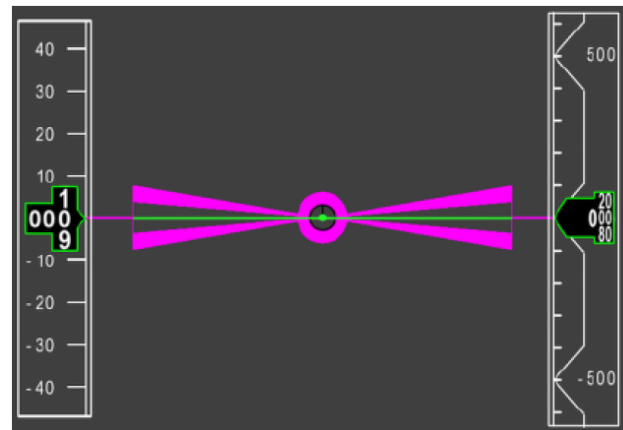


Fig. 42. Bowtie display for Sum-of-Sines Tracking and Attitude Capture and Hold tasks (reproduced from Ref. 8)

Pitch/Roll Sum-of-Sines Tracking

The objectives of the Sum-of-Sines (SOS) Tracking MTE (Ref. 8) are to evaluate the handling qualities in forward flight in a tight, closed-loop tracking task, evaluate the feel system, control sensitivity, and cross coupling, and identify any bobble or PIO tendencies.

The task is driven by an automated command signal based on a sum of sine waves of different frequency

and amplitudes. A Fibonacci series-based SOS input is defined to emphasize a frequency range that encompasses key vehicle dynamics and typical closed-loop control (Ref. 8). In this case, the sine wave magnitudes were set via a second order Butterworth filter with a bandwidth of $\omega_{BW} = 0.60$ rad/sec for the pitch axis and $\omega_{BW} = 0.83$ rad/sec for the roll axis. The magnitudes of the sine waves were scaled to give a pitch target signal RMS of 2.5 deg and a roll target signal RMS of 10 deg.

Table 8 lists the desired and adequate performance criteria for the Pitch/Roll Sum-of-Sines Tracking tasks.

Break Turn

The Break Turn MTE (Ref. 9) is a non-precision, aggressive maneuver composed of a 90 deg heading change designed for evasive combat maneuvering. The pilot must perform an aggressive flight path change within the operation flight envelope (OFE) of the aircraft. The task is meant to investigate any potential handling qualities issues or cliffs or pilot induced oscillation (PIO) tendencies resulting from aggressive roll-axis inputs. To increase pilot workload, the amount of altitude and airspeed loss allowed is specified.

The time requirement to complete the 90 deg heading change is based on an ideal time to complete the maneuver T_{ideal} and an allowable ΔT . Calculation of T_{ideal} is explained in Ref. 9, and is based on several parameters. For both aircraft used in this study, T_{ideal} was calculated using the MIL-STD-1797B Class I, Category A time to bank requirements of $\phi_{req} = 60$ deg in $t_{req} = 1.3$ sec, a task velocity of $V = 180$ kts, and an aircraft normal load factor limit $n_{z_{lim}} = 2.5$ g. The resulting $T_{ideal} = 8.9$ sec, giving the following desired and adequate times:

$$T_{des} = T_{ideal} + 3.5 \text{ sec} = 12.4 \text{ sec} \quad (17)$$

$$T_{adq} = T_{ideal} + 7.0 \text{ sec} = 15.9 \text{ sec} \quad (18)$$

Table 9 lists the desired and adequate performance criteria for the Break Turn task.

High-Speed Acceleration/Deceleration

The High-Speed Acceleration/Deceleration MTE (Ref. 10) evaluates up-and-away handling qualities in

transitional flight for aircraft that experience significant configuration changes with airspeed. The maneuver is composed of two phases: a maximum performance level-flight acceleration, and a maximum performance level-flight deceleration, over a speed range of $V = 50$ kts to $V = V_H - 10$ kts. In the case of the generic coaxial-pusher and tiltrotor aircraft tested here, the airspeed range used was $V = 50 - 220$ kts. Each of the phases has separate performance criteria and is rated separately.

The objectives of the MTE are to evaluate pitch and heave axis handling qualities for aggressive maneuvering throughout the speed range envelope; check for undesirable coupling between the longitudinal, lateral-directional, and unconventional axes; check for controller harmony between the heave axis, pitch axis, and unconventional/auxiliary control axes/inceptors; and check for handling qualities degradation during transitional flight regimes.

Like the Break Turn MTE described above, there is an ideal or minimum time to complete the maneuver ($T_{minimum}$) that must be determined prior to testing. In this case, $T_{minimum}$ was determined during testing by having pilots fly the acceleration and deceleration portions of this task, using the tolerances given in Table 10 as a guide only (but not adhering to them strictly). The following values of $T_{minimum}$ were determined for the coaxial-pusher:

$$\text{Acceleration: } T_{minimum} = 36 \text{ sec} \quad (19)$$

$$\text{Deceleration: } T_{minimum} = 46 \text{ sec} \quad (20)$$

and for the tiltrotor:

$$\text{Acceleration: } T_{minimum} = 36 \text{ sec} \quad (21)$$

$$\text{Deceleration: } T_{minimum} = 34 \text{ sec} \quad (22)$$

Table 10 lists the desired and adequate performance criteria for the High-Speed Acceleration/Deceleration task.

Table 7. Pitch/Bank Angle Capture and Hold Performance Criteria

	Desired	Adequate
<i>Pitch</i>		
<ul style="list-style-type: none"> • Pitch angle error (from command) tolerance: • Airspeed deviation tolerance: • No more than one pitch attitude overshoot on the initial capture of each attitude. Magnitude of overshoot is less than: • PIO considerations: • Inter-axis coupling shall not be 	<ul style="list-style-type: none"> ±1 deg ±5 kts 1 deg No PIO tendencies Undesirable 	<ul style="list-style-type: none"> ±2 deg ±10 kts 2 deg No divergent PIO tendencies Objectionable
<i>Roll</i>		
<ul style="list-style-type: none"> • Bank angle error (from command) tolerance: • Airspeed deviation tolerance: • No more than one bank angle overshoot on the initial capture of each attitude. Magnitude of overshoot is less than: • PIO considerations: • Inter-axis coupling shall not be 	<ul style="list-style-type: none"> ±5 deg ±5 kts 5 deg No PIO tendencies Undesirable 	<ul style="list-style-type: none"> ±10 deg ±10 kts 10 deg No divergent PIO tendencies Objectionable

Table 8. Pitch/Roll Sum-of-Sines Tracking Performance Criteria

	Desired	Adequate
<i>Pitch</i>		
<ul style="list-style-type: none"> • Remain within ±1 deg for X percent of the time • Remain within ±2 deg for X percent of the time • PIO Considerations: • Inter-axis coupling shall not be 	<ul style="list-style-type: none"> 50 % - No PIO tendencies Undesirable 	<ul style="list-style-type: none"> - 75 % No divergent PIO tendencies Objectionable
<i>Roll</i>		
<ul style="list-style-type: none"> • Remain within ±5 deg for X percent of the time • Remain within ±10 deg for X percent of the time • PIO Considerations: • Inter-axis coupling shall not be 	<ul style="list-style-type: none"> 50 % - No PIO tendencies Undesirable 	<ul style="list-style-type: none"> - 75 % No divergent PIO tendencies Objectionable

Table 9. Break Turn Performance Criteria

	Desired	Adequate
<ul style="list-style-type: none"> • Complete maneuver within time $T < \Delta T + T_{ideal}$ • Final change in directional flight path shall be at least 85 deg and no more than X degrees • When rolling out to wings-level attitude, the overshoot in roll attitude shall not exceed X degrees • Final airspeed loss shall be no more than X% of initial airspeed ($0.8V_H$) • Maintain altitude within ±X feet • Any oscillations or interaxis coupling shall not be 	<ul style="list-style-type: none"> $\Delta T = 3.5$ sec 95 deg 5 deg 10% 75 ft Undesirable 	<ul style="list-style-type: none"> $\Delta T = 7.0$ sec 105 deg 10 deg 20% 150 ft Objectionable

Table 10. High-Speed Acceleration/Deceleration Performance Criteria

	Desired	Adequate
• Complete acceleration within time $T < \Delta T + T_{\text{minimum}}$	$\Delta T = 8.0 \text{ sec}$	$\Delta T = 15.0 \text{ sec}$
• Complete deceleration within time $T < \Delta T + T_{\text{minimum}}$	$\Delta T = 10.0 \text{ sec}$	$\Delta T = 20.0 \text{ sec}$
• Final airspeed to be captured within:	$\pm 2 \text{ kts}$	$\pm 3 \text{ kts}$
• Maintain altitude within X feet of initial altitude:	$\pm 100 \text{ ft}$	$\pm 150 \text{ ft}$
• Maintain heading within X degrees of initial heading:	$\pm 5 \text{ deg}$	$\pm 10 \text{ deg}$
• Maintain bank angle (from trim) within:	$\pm 5 \text{ deg}$	$\pm 10 \text{ deg}$
• Any oscillations or inter-axis coupling shall not be:	Undesirable	Objectionable
• Control harmony between axes shall not be:	Undesirable	Objectionable
• Rotor RPM shall remain within the limits of X without undue pilot compensation:	OFE	SFE